Faculty of Sciences and Applied Sciences
Department of Mechanical Engineering

END OF STUDY PROJECT

Presented for the attainment of the master's degree in mechanical engineering
Option: Energetics

Subject

Numerical investigation of magneto hydrodynamic (MHD) hybrid nanofluid flow between two coaxial cylinders.

By:

LARIK ABDERRAHMANE

Public defense / /2024 before the jury composed

President: Dr.**Aghbari**	University of Bouira
Promoter: Pr. Mahfoud Brahim	University of Bouira
Examiner: Dr.**Messai**	University of Bouira

2023/2024

الجمهورية الجزائرية الديمقراطية الشعبية
République Algérienne Démocratique et Populaire

وزارة التعليم العالي والبحث العلمي
جامعة أكلي محند أولحاج
- البويرة -
كلية العلوم والعلوم التطبيقية

Ministère de l'Enseignement Supérieur
et de la Recherche Scientifique
Université Akli Mohand Oulhadj - Bouira -
ⵜⴰⵙⴷⴰⵡⵉⵜ ⴰⴽⵍⵉ ⵎⵓⵃⴻⵏⴷ ⵓⵍⵃⴰⵊ - ⵜⵉⴱⵡⵔⵉⵔⵉⵏ -
Faculté des Sciences et des Sciences Appliquées

Génie mécanique

Spécialité : Energétique

Autorisation de déposer un mémoire de Master pour soutenance

Je soussigné, l'enseignant (e) : ……Pr.Mahfoud Brahim

L'encadreur du mémoire de fin d'études des étudiants :

1- LARIK ABDERRAHMANE

Ayant le mémoire de fin d'études de Master intitulé : Numerical investigation of magneto hydrodynamic (MHD) hybrid nanofluid flow between two coaxial cylinders.

Promotion : 2023/ 2024

Et après voir et consulté le mémoire dans sa forme finale j'autorise les étudiants à l'imprimer et la déposer pour la soutenance.

Bouira le : 13/06/2024

Signature du L'encadreur

Signature du chef de département

الجمهورية الجزائرية الديمقراطية الشعبية
Republique Algerienne Democratique et Populaire

وزارة التعليم العالي و البحث العلمي
جامعة أكلي محند أولحاج - البويرة

Ministère de l'Enseignement Supérieur
et de la Recherche Scientifique
Université Akli Mohand Oulhadj - Bouira
Tasdawit Akli Muhend Ulḥağ - Tubirett

نموذج التصريح الشرفي الخاص بالالتزام بقواعد النزاهة العلمية لإنجاز بحث.

انا الممضي اسفله،

السيد(ة) ..... الصفة: طالب، استاذ، باحث .....

الحامل(ة) لبطاقة التعريف الوطنية: ..... والصادرة بتاريخ .....

المسجل(ة) بكلية / معهد ..... قسم .....

والمكلف(ة) بإنجاز اعمال بحث(مذكرة، التخرج، مذكرة ماستر، مذكرة ماجستير، اطروحة دكتوراه).

عنوانها .....

تحت إشراف الأستاذ(ة): .....

أصرح بشرفي اني ألتزم بمراعاة المعايير العلمية والمنهجية الاخلاقيات المهنية والنزاهة الاكاديمية المطلوبة في انجاز البحث المذكور أعلاه.

التاريخ: .....

توقيع المعني(ة)

رأي هيئة مراقبة السرقة العلمية:

النسبة: 18 %

الامضاء:

جامعة أكلي محند اولحاج - البويرة
كلية العلوم و العلوم التطبيقية
قسم الهندسة الميكانيكية
مكلف بالتدريس و التعليم في التدرج

ACKNOWLEDGMENTS

We thank almighty god for giving us the strength, courage, and patience to begin and complete this modest work.

First, this work would not be as rich and could not have come to fruition without the help and guidance of Mr. MAHFOUD Brahim. We thank him for the exceptional quality of his supervision, patience, rigour, and availability during our preparation of this thesis.

Our thanks also go to all our professors in the Mechanical Engineering Department at the University of BOUIRA for their generosity and great patience despite their academic and professional commitments.

Finally, I sincerely thank everyone who, directly or indirectly, contributed to the completion of this work.

Dedication

I dedicate this work to:

The one whose heart saw me before her eyes and whose innermost being embraced me before her hands did.

The source of tenderness is my mother, my mother, and then my mother, May Almighty God welcome you into His vast paradise.

To the source of strength and seriousness, the one who gave me love, respect, and good character, my father, May Almighty God welcome you into His vast paradise.

To my brothers: Mohamed, Ahmed, Malek, Fathi,

And sisters: Hayet and Ilham, all my friends, and the energetic group.

Finally, I dedicate this to all the people who love whom I love and me.

Abderrahmane

Abstract

A numerical investigation was conducted to analyse the flow characteristics of a hybrid nanofluid rotating through an annulus formed within a coaxial cylinder. This study compares the thermal performance of the hybrid nanofluid (composed of graphene oxide (GO), copper (Cu), and kerosene oil) with the base fluid (kerosene). A radial magnetic field was applied to examine its impact on flow and heat transfer characteristics. The mathematical model, formulated as ordinary differential equations, was solved using the finite volume method. Graphical representations were used to analyse azimuthal velocity, temperature, and Nusselt number under increasing magnetic intensity. The results indicated that a higher magnetic Hartmann number led to an increase in the distribution of temperature and azimuthal velocity in the middle of the annulus. The findings also highlighted that electromagnetic damping is more advantageous for the hybrid nanofluid than for (Cu/kerosene oil).

Keywords: *Hybrid nanofluid (GO + Cu/kerosene oil), nanofluid (Cu/kerosene oil), coaxial cylinders, magnetic field, Nusselt number.*

ملخص:

تم إجراء بحث عددي (رقمي) لتحليل خصائص التدفق لمائع نانوي هجين يدور خلال حلقة متكونة داخل أسطوانة متحدة المحور .تقارن هذه الدراسة الأداء الحراري للسائل النانوي الهجين (المكون من أكسيد الغرافين(GO) ، والنحاس (Cu)، وزيت الكيروزين) مع السائل الأساسي (الكيروزين) .تم تطبيق مجال مغناطيسي شعاعي لفحص تأثيره على خصائص التدفق وانتقال الحرارة .تم حل النموذج الرياضي، الذي تمت صياغته كمعادلات تفاضلية عادية، باستخدام طريقة الحجم المحدود .تم استخدام التمثيلات البيانية لتحليل السرعة السمتية ودرجة الحرارة وعدد نسلت في ظل زيادة الكثافة المغناطيسية .أشارت النتائج إلى أن ارتفاع رقم هارتمان المغناطيسي أدى إلى زيادة في توزيع درجة الحرارة والسرعة السمتية في منتصف الحلقة .أبرزت النتائج أيضًا أن التخميد الكهرومغناطيسي أكثر فائدة للموائع النانوية الهجينة من النانو المكون من (النحاس / زيت الكيروزين)

الكلمات المفتاحية: الموائع النانوية الهجينة(النحاس+الغرافين/ زيت الكيروزين)، الموائع النانوية (النحاس/ زيت الكيروزين)، الأسطوانات المحورية، المجال المغناطيسي، رقم نسلت.

Résumé:

Une étude numérique a été menée pour analyser les caractéristiques d'écoulement d'un nanofluide hybride tournant à travers un anneau formé dans un cylindre coaxial. Cette étude compare les performances thermiques du nanofluide hybride (composé d'oxyde de graphène (GO), de cuivre (Cu) et d'huile de kérosène) avec le fluide de base (kérosène). Un champ magnétique radial a été appliqué pour examiner son impact sur les caractéristiques d'écoulement et de transfert de chaleur. Le modèle mathématique, formulé sous forme d'équations différentielles ordinaires, a été résolu en utilisant la méthode des volumes finis. Des représentations graphiques ont été utilisées pour analyser la vitesse azimutale, la température et le nombre de Nusselt sous une intensité magnétique croissante. Les résultats ont indiqué qu'un nombre de Hartmann magnétique plus élevé entraînait une augmentation de la distribution de la température et de la vitesse azimutale au milieu de l'anneau. Les résultats ont également mis en évidence que l'amortissement électromagnétique est plus avantageux pour le nanofluide hybride que pour (Cu/ huile kérosène).

Mots clés : Nanofluid hybride (GO + Cu/huile de kérosène), nanofluid (Cu/huile de kérosène), cylindres coaxiaux, champ magnétique, le nombre de Nusselt.

Summary

List of Figures

List of tables

Nomenclature:

R: cylinder radius [m].

H: cylinder height [m].

T: Temperature [K].

Tc: Cold disk temperature [K].

Th: Hot disk temperature [K].

B: magnetic field.

Lc: characteristic length.

$\mathbf{e_r}$, $\mathbf{e_z}$, $\mathbf{e_\theta}$**:** The unit vectors of the radial, axial, and azimuthal directions respectively.

$\boldsymbol{f'_{Lr}}$, $\boldsymbol{f'_{Lz}}$, $\boldsymbol{f'_{L}}$**:** the components of the radial, axial, and azimuthal Lorentz electromagnetic force (N. m-3).

$\mathbf{F_{Lr}}$**, FLz, FL** : Dimensionnels Lorentz forces in radial, axial and azimutal directions.

J: *Volumetric current density (A.* m^{-3}*).*

$\mathbf{J_r}$,$\mathbf{J_z}$,$\mathbf{J_\theta}$ **:** Dimensionless electric currents in radial, axial and azimuthal directions.

Pr: The Prandtl number.

Re: Reynolds number.

Ri: Richardson number.

Ha: Hartmann number.

Gr: Grashof number.

Ra: Rayleigh number.

Nu : nombre de Nusselt.

$\overline{Nu}$ **:** Average Nusselt number.

P: pressure [$N.m^{-2}$].

t: Time [s].

$\mathbf{C_P}$**:** Specific heat at constant pressure [$J.kg^{-1}.K^{-1}$].

$\boldsymbol{\Gamma_\Phi}$*:* the diffusion coefficient.

$\mathbf{S_\Phi}$**:** the source term.

K: thermal conductivity [$w.\ m^{-1}.\ K^{-1}$].

V: volume [m^3].

m: the mass [kg].

Kr: rotation parameter.

V: axial speed.

U, v, w: the velocity components in the radial, axial, and azimuthal directions.

Δx**:** variation of x. [m].

Δy**:** variation of y [m].

Greek symbols:

α: Thermal diffusivity [$m^2.s^{-1}$].

β: Thermal expansion coefficient at constant pressure [K^{-1}].

μ: Dynamic viscosity [kg. $m^{-1}.s^{-1}$].

ν: Kinematic viscosity [$m^2.s^{-1}$].

ρ: Density [kg. m^{-3}].

Ψ: Dimensionless current function.

Δ**T:** the temperature difference.

θ: Dimensionless temperature.

Ω: angular speed.

φ: volume fraction.

ϕ: dependent variable.

ω : Vorticity.

σ : electrical conductivity [$\Omega^{-1}.m^{-1}$].

Φ**:** Dimensionless electric potential.

The clues:

nf: Nanofluid.

hnf: hybrid Nanofluid.

P: particle.

f: basic fluid.

Max: maximum.

i: following direction x.

j: following the y direction.

GENERAL INTODUCTION

General Introduction

In the expansive domain of fluid mechanics, the intricate interplay between nanofluids and their behaviour over distinct geometries has been the focus of scholarly investigations. The existing body of literature reveals a discernible trend wherein nanofluids have been meticulously scrutinized in the context of their flow over stretched surfaces and cylindrical structures. A conspicuous omission, however, lies in the absence of a comprehensive exploration of the dynamics of hybrid nanofluids within the confined space between two coaxial cylinders.

In addressing this discernible research gap, our study embarks on a nuanced examination of the intricate fluid dynamics involving a hybrid nanofluid composed of Graphene Oxide (GO) and Copper nanoparticles suspended in Kerosene oil, alongside a conventional nanofluid featuring Copper nanoparticles dispersed in Kerosene oil. The encapsulation of these nanofluids between two coaxial cylinders unfolds a novel dimension in the understanding of heat transfer phenomena.

The investigation extends beyond the conventional, integrating the impact of magnetic fields through Magnetohydrodynamics (MHD) and accounting for Joule heating effects, thereby augmenting the scientific rigour of the analysis. Mathematical modelling serves as the backbone of our inquiry, allowing us to delineate the governing equations in a manner that encapsulates the complexities inherent in the problem.

Through a meticulous transformation process, the ordinary differential equations (ODEs) governing the fluid dynamics are rendered into a dimensionless form, facilitated by the judicious selection of pertinent variables.

The elucidation of results transcends conventional presentations, adopting a graphical representation to unravel the intricate influences of sundry variables on key fluidic parameters. The comprehensive analysis spans velocity profiles, pressure distributions, fluid temperature gradients, Nusselt numbers, and skin friction coefficients.

This undertaking not only augments the existing body of scientific knowledge surrounding nanofluid dynamics but also marks a pioneering exploration into the uncharted territory of hybrid nanofluids confined between coaxial cylinders.

The amalgamation of theoretical rigour, numerical precision, and graphical elucidation renders this study a significant contribution to the burgeoning field of fluid dynamics and nanotechnology.

In this study, we will particularly focus on studying the flow of hybrid nanofluids between two coaxial cylinders. The inner cylinder is fixed while the external cylinder has a rotation. A uniform magnetic field is taken along the radial direction to examine the characteristics of the flow and heat transfer. The finished volume method is used to separate and resolve energy equations by the finished volume method. This study was divided into four chapters organized as follows:

- The first chapter is devoted to the presentation of generalities on nanofluids, nanofluids, hybrids, and Magneto-Hydrodynamics (MHD). As well as a bibliographic synthesis of various works published on nanofluids and their development.
- The second chapter of the intensity sports model, dynamic viscosity, thermal capacity, extension coefficient, conductivity, electrical conductivity with the sports formula of the problem and the governing equations as well as the border conditions, then three dimensions (r, θ, z).
- The third chapter is devoted to the presentation of the finite volume method, its implementation for the discretization of the equations of the problem as well as the choice of the appropriate mesh.
- In chapter four, we bring together the validation of the results as well as the main numerical results of this study. Comments, interpretations, and analyses of the various results of this parametric study are also presented.
- Finally, we end this report with a general conclusion, summarising the main results obtained.

Chapter I.
Bibliographic reviews

Chapter I. Bibliographic Reviews

I.1 Introduction:

In recent years, there have been significant advancements in energy systems within the industrial sector, resulting in the generation of extremely high heat flux. Traditional coolants such as water, ethylene glycol, and oils prove ineffective in managing such elevated heat levels. To enhance the thermal properties of fluids, a novel approach involves introducing solid particles with excellent thermal characteristics and nanometre size into the base fluid. This groundbreaking fluid is termed "Nano fluid." Coined by Choi in 1995 at the Argonne National Laboratory in the United States, the term continues to be widely used to characterize this unique colloidal suspension. Nanofluids exhibit superior heat transfer properties compared to conventional fluids, making them invaluable in industrial applications operating in high-temperature environments.

In this chapter, we will talk about a numerical study of magneto-hydro-dynamic hybridization (MHD). Nanofluid flow between two combined cylinders.

I.2 Bibliographic review:

Warming or cooling liquids are of major significance to numerous mechanical divisions, including transportation, vitality supply and generation, and hardware. The warm conductivity of these liquids plays an imperative role in the advancement of energy-efficient warm exchange hardware. Nevertheless, routine warm-exchange liquids have destitute warm-exchange properties compared to most solids. [2]For example, the warm conductivity of copper at room temperature is 700 times more noteworthy than that of water and 3000 times more noteworthy than that of motor oil, as appears in Table 1. The warm conductivity of metallic fluids is much more prominent than that of nonmetallic liquids [1]. Hence, the warm conductivities of liquids that contain suspended, strong metallic particles are anticipated to be essentially improved when compared with conventional warm exchange fluids. [1]. In truth, various hypothetical and exploratory ponders of the compelling warm conductivity of scatterings that contain strong particles have been conducted since Maxwell's hypothetical work was distributed more than 100 years prior (Maxwell, 1881). However, all of the ponders on the warm conductivity of suspensions have been kept to millimetre- or micrometer-measured particles.[1].

On the premise of this verifiable foundation, it was proposed that if nanometer-sized particles can be suspended in conventional warm exchange liquids, an unused course of designed liquids with high warm conductivity may be produced.9 These so-called "Nano fluids" are anticipated to display prevalent properties relative to those not only of ordinary

warm exchange liquids but also of liquids containing micrometre-sized metallic particles. Since the surface-area-to-volume proportion is 1000 times bigger for particles with a 10 nm breadth than for particles with a 10 mm breadth, a much more emotional advancement in successful warm conductivity is anticipated because of diminishing the molecule measure in a suspension [2]. Analysts at the Argonne National Research Facility (ANL) have been creating advanced liquids for mechanical applications, counting area warming and cooling frameworks (Choi and Tran, 1991; Choi et al., 1992a and 1992b). One of the issues distinguished in this R&D program was that micrometre-sized particles cannot be utilized in viable warm exchange hardware because of serious clogging problems; however, Nanophase metals are accepted to be in a perfect world suited for applications in which liquids stream through small sections since the metallic nanoparticles are small enough that they are anticipated to act like particles of the fluid. Hence, nanometer-sized particles will not clog stream entries but will move forward the warm conductivity of the liquids. This will open up the plausibility of utilizing nanoparticles in a microchannel for numerous imagined high-heat-load applications [1].

Several research into heat transfer have been carried out over the previous decades to develop new techniques for improving transfer performance through the use of metallic or non-metallic additives to base fluids to increase their thermal conductivity[4].

To predict the thermal conductivity of Nano-fluids, many theoretical models have been developed recently. However, there is still controversy over the interpretation of the thermal conductivity enhancement of Nanofluids. Thus, none of the theoretical models developed can completely explain the improvement in thermal conductivity in Nano-fluids. On the other hand, some researchers have reported experimental data on thermal conductivity, which is compatible with the predictions of classical models (such as the Hamilton and Crosser model [5]). For research involving heat transfer and the properties of Nanofluids, reference should be made to the studies of Eastman et al. [6], Maïga et al. [7] and Wang and Mujumdar [8].

Nano-fluids are then one of the fruits of such richness. Equipped with particular and interesting physicochemical properties, such as their significant thermal conductivity, Nano-fluids offer a heat transfer coefficient unbeatable by other heat transfer agents. The studies carried out in this new direction have provided a rich but very varied bibliography: although the majority are quite positive.

Oztopet al. [9] studied the effect of using different Nano-fluids on the distribution of the temperature field in an enclosure filled with a mixture of water and Nano-fluid. They demonstrated that increasing the value of the Rayleigh number; the heater size and the volume fraction of Nano-fluids improves heat transfer.

Bhattadet al (2017)[10] summarized research on the preparation and characterization of Nanofluids, and various thermophysical and electrical properties (density, heat capacity, viscosity, thermal conductivity, surface tension, electrical conductivity, freezing characteristics, etc.) Nanofluids. The applications of Nanofluids in refrigeration systems as refrigerators, lubricants, and secondary fluids are well grouped and discussed. Finally, challenges and opportunities for future research are identified, which will be useful for newcomers and manufacturers in this field.

Table I-1 THERMAL CONDUCTIVITY (W/m-K) OF VARIOUS MATERIALS AT 300 K.

Material	Thermal Conductivity
Metallic Solids	
Silver	429
Copper	401
Aluminum	237
Nonmetallic Solids	
Silicon	148
Metallic Liquids	
Sodium @ 644 K	72.3
Nonmetallic Liquids	
Water	0.613
Engine oil	0.145

I.3 Nanofluids:

I.3.1 Definition of Nanofluids:

Nanofluids are designed as colloids made up of a base liquid and nanoparticles Nanoparticles have warm conductivities, ordinarily an order of magnitude higher than those of the base liquids, and sizes altogether less than 100 nm. The presentation of nanoparticles upgrades the warm exchange execution of the base liquids altogether. The base liquids may be water, natural fluids (e.g., ethylene, ethylene glycols, refrigerants, etc.), oils and oils, bio-fluids, polymeric arrangements, and other common fluids. The nanoparticle materials incorporate chemically steady metals (e.g., gold, copper), metal oxides (e.g., alumina, silica, zirconia, Titania), oxide ceramics (e.g., Al2O3, CuO), metal carbides (e.g., SiC), metal nitrides (e.g., AIN, SiN), carbon in different shapes (e.g., precious stone, graphite, carbon nanotubes, fullerene), and functionalized nanoparticles [3].

- **nanoparticles:**

Ultrafine particles (UFP) or nanoparticles are atoms with sizes extending from one to 100 nanometers (one nm = 10-9 m = 0.000000001 m). They are, hence, smaller than cells and bigger than molecules.

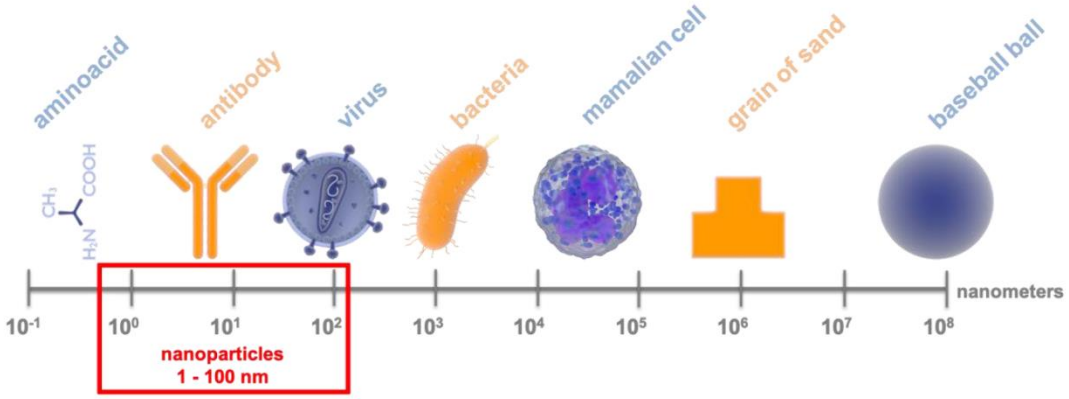

Figure I. 1 Comparison of nanoparticle size to other objects; presented on a logarithmic scale.

There are various ways to plan nanoparticles, but they drop into two bunches:

Physical forms, such as mechanical pounding.

In chemical forms, such as pyrolysis or chemical precipitation the nanoparticles most utilized to get nanofluids are:

- Metal oxide nanoparticles :
  - Aluminium oxide (Al2O3)
  - Copper oxide (CuO)
  - Silicon oxide (SiO2)
  - Titanium oxide (TiO2)
- Metal nanoparticles:
  - Aluminum (Al)
  - Copper (Cu)
  - Gold (Ag)
- Non-metallic nanoparticles :
  - Carbone nanotube (CNT), Diamante
  - Refrigeration liquids (R12, R22)

Table I-2 Thermo-physical properties of different materials.

	Nanoparticle and base fluid	K (W /mK)	ρ(Kg/m3)	Cp (J/ Kg K)	μ (Pa.s)
Metallic (solid)	**Cu** **Fe** **Ni** **Au** **Ag** **C (diamond)**	**400** **80,2** **90,7** **317** **429** **2300**	**8954** **7870** **8900** **19,300** **10,500** **3500**	**383** **447** **444** **129** **235** **509**	
Metal Oxide (solids)	**SiO2** **TiO2** **Al2O3** **Cu O** **SiC**	**1,38** **8,4** **36** **69** **490**	**2220** **4157** **3970** **6350** **3160**	**745** **710** **765** **535** **675**	
Non-metallic liquids	The water Ethylene glycol (EG)	**0,613** **0,258**	**1000** **1132**	**4183** **2349**	**0,0008** **5130,0157**

The basic fluids known in the literature are:

The water:

- Ethylene and propylene glycol.
- Oils and other lubricants.
- Toluene.
- Fluid woods.

I.3.2 PREPARATION OF NANOFLUIDS:

The initial and crucial step in experimental studies involving nanofluids is the preparation process. Nanofluids are more than simple liquid-solid mixtures; they require specific conditions such as a uniform and stable suspension, lasting suspension, minimal particle agglomeration, and no chemical alteration of the fluid. The production of Nanofluids involves dispersing nanometer-scale solid particles into base liquids like water, ethylene glycol (EG), oils, etc. However, agglomeration poses a significant challenge during Nano fluid synthesis.

Two primary techniques are commonly employed for Nanofluid production: the single-step method and the two-step method. [1].

- **one-step :**

The one-step method for creating Nanofluids containing metallic particles was utilized. This procedure includes the coordinated condensation of metallic vapour into nanoparticles by contact with a streaming moo vapour-weight fluid.

- **two-step :**

The two-step strategy is broadly utilised within the generation of Nanofluids, considering the commercially accessible Nano powders given by different companies. In this approach, nanoparticles are synthesized and then scattered into the base liquids. Ordinarily, ultrasonic hardware is utilized to guarantee the careful scattering of particles and relieve agglomeration. In comparison to the single-step strategy, the two-step method is especially effective with oxide nanoparticles but may experience challenges when managing metallic particles.

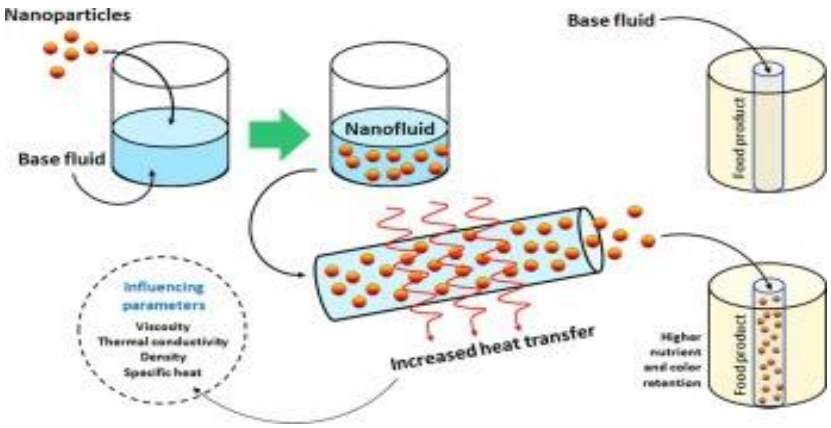

Figure I. 1 PREPARATION OF NANOFLUIDS.

I.3.3 APPLICATION OF NANOFLUIDS:

- **The industry:**

Industries in general (heat engines, air conditioners, power components, nuclear devices, particle accelerators, aviation or aerospace services, etc.) because they minimize the amount of cooling equipment or its size of Electrical power, as it increases our productivity without causing fatigue. The estimate is it takes ten times the pump's power, or enormous and unprofitable, to twice the exchange coefficient. Improvements in Nanofluids can help somewhat mitigate this. As much as 80% of the coefficient can be achieved under turbulent conditions without affecting the amount of power needed for operation [11].

- **Cooling of electronic systems:**

Numerous investigations have been conducted on the topic of cooling in open cavities using Nanofluids, as demonstrated by Hamdi et al. [12] The current study examines the heat transmission of water Nanofluids (Cu, Ag, Al2O3, and TiO2) in a cavity and the flow of two-dimensional mixed convective fluids. Powered by a digital search that is partially heated from below and has caps on both sides. On the wall, there are two separate heat sources. On the other hand, the ceiling, vertically adjustable walls, and lower housing are all kept at a constant temperature by cooling systems. Remain apart from the lower wall's remaining edge.

- **Cooling of thermal systems:**

Primarily utilized for impact and cooling energy systems the impact of form factor on fluid flow upward motion this argument is supported by research conducted by multiple research organizations in Bara et al. The outcome of the Nano fluid's spontaneous convection in a closed cavity filled with it is both pure water and a mixture of water and nanoparticles (Cu) at the same time. To alter them Rayleigh counts [13].

- **Cooling of military systems:**

Directed energy weaponry and cooling power electronics are two examples of military usage. It has been demonstrated that the latter, which uses large heat fluxes (q > 500 to 1000 W/cm2) or Nanofluids, is efficient in cooling these and other military equipment, such as high-power laser diodes and military vehicles. [11].

- **Cooling of nuclear systems:**

The only multidisciplinary centre at MIT is dedicated to new nanotechnology Nanofluid, which is employed in the nuclear power sector. The possible effects of using Nanofluids on the safety and financial viability of nuclear and neutronic systems are currently being assessed [11].

- **biomedicine:**

In biological science, Nanofluids and nanoparticles are used. For instance, iron-based nanoparticles have been used as medication carriers to reduce some of the negative effects of conventional cancer treatments. Moreover useful for safer surgery and provides efficient cooling approximately the surgery site. When it comes to cooling high-power laser and x-ray mirrors, targets, and filters, Nanofluids can offer an appealing alternative.

I.3.4 Advantages and disadvantages:

I.3.4.1 Advantages of Nanofluids:

However, Nanofluids have the following advantages:

- the surface area for heat transfer between the fluid and the particles is substantial. To achieve an increase in heat transfer, the volume is decreased.
- In contrast to conventional liquids, it minimizes fouling particles, which facilitates the system's downsizing.
- Tunable characteristics, such as surface wettability and heat conductivity, that vary depending on the application of various particle concentrations.

I.3.4.2 Disadvantages of Nanofluids:

- The results obtained by various researchers lack coherence

There is a theoretical lack of understanding of the mechanism causing performance changes Suspension characteristics are poor. Stability of nanoparticle dispersions. Amplification of charge loss and pumping power.

- Higher viscosity and lower specific heat.
- The high cost of Nanofluids. Challenges in the production process [11].

I.4 Hybrid Nanofluids:

I.4.1 Definition of hybrid Nanofluids:

Hybrid Nanofluid is a new class of heat transfer fluid with the potential to achieve higher heat transfer performance than single nanoparticle Nanofluids and traditional cooling fluids (ethylene glycol and water). Numerous review studies have examined the synthesis and consistency of hybrid nanoparticles, and it is widely known that these particles are significant in several manufacturing and technological domains. A suitable blend of nanoparticles is one of the most crucial factors to consider while making a long-lasting hybrid Nanofluid. Metal nanoparticles (Ag, Cu), metal oxides (Al2O3, CuO, and Fe2O3), carbon materials (graphite, MWCNTs, CNTs), metal carbide, and metal nitride were the most commonly found types of nanoparticles.

In addition, the composition of the nanoparticles as well as their size, form, and solid volume fractions play crucial roles in maximizing the hybrid Nano fluid's thermal conductivity. [22].

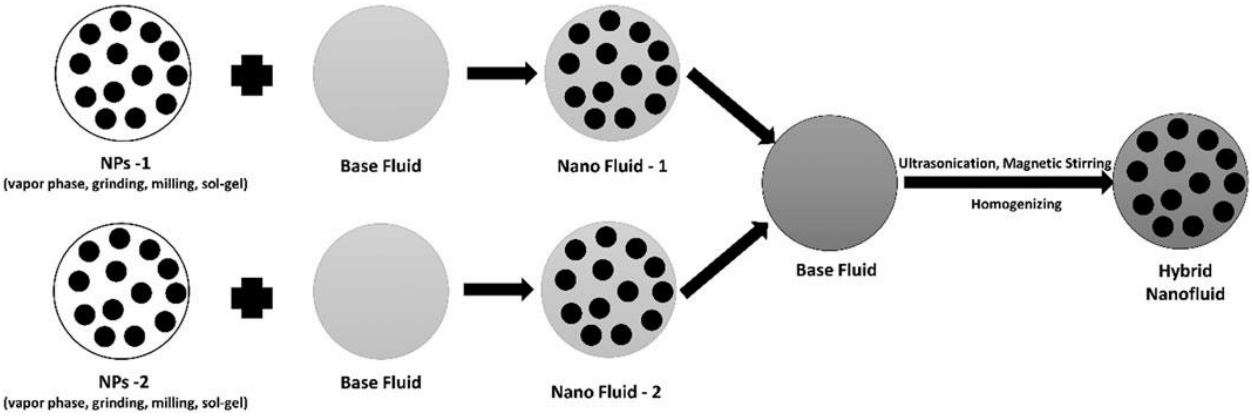

Figure I. 2. Schematic illustration of two-step synthetic approach.

I.5 Magneto-hydrodynamics (MHD)

I.5.1 Definition of MHD:

Magneto-hydrodynamics (MHD) is the study of the dynamics of electrically conducting fluids in the presence of a magnetic field. It consists of three words magneto, hydro, and dynamics, which mean magnetic effects, water, and movement. This field combines principles from both magnetism and fluid dynamics and has applications in various engineering and scientific disciplines.

I.5.2 Applications of Magneto-Hydrodynamics (MHD):

Magneto-Hydrodynamics (MHD) combines principles of both magnetism and fluid dynamics to study the behaviour of electrically conducting fluids in the presence of magnetic fields. This interdisciplinary field has a wide range of applications across various scientific and engineering domains. Here are some notable applications of MHD:

I.5.2.1 Industrial Processes:

- **Metallurgy:**

MHD is used in processes like electromagnetic stirring, where magnetic fields are applied to molten metals to improve mixing and solidification, enhancing material properties.

- **Electromagnetic Casting:**

Involves using MHD to control the shape and cooling rate of molten metal during casting, leading to higher-quality products with fewer defects.

I.5.2.2 Energy Generation:

MHD generators convert thermal or kinetic energy directly into electrical energy using a conducting fluid (like plasma) moving through a magnetic field. These generators offer high efficiency and fewer moving parts compared to traditional turbines.

I.5.2.3 Cooling Systems:

- **Nuclear Reactor Cooling:**

MHD is used to enhance heat transfer in nuclear reactors by using liquid metals or other conducting fluids as coolants, improving safety and efficiency.

- **Electronics Cooling:**

MHD cooling systems can be applied to remove heat from high-performance electronic devices, using conducting fluids that circulate under the influence of magnetic fields to dissipate heat more effectively.

I.5.2.4 Marine Propulsion:

MHD is used to develop propulsion systems for ships and submarines, where a conducting fluid (usually seawater) is accelerated by a magnetic field to create thrust. This method offers silent and efficient propulsion, making it ideal for military applications.

I.5.2.5 Medical Applications :

- **Magnetic Drug Targeting:**

MHD can be applied in targeted drug delivery systems, where magnetic fields are used to direct drug-loaded magnetic nanoparticles to specific locations within the body.

I.6 Conclusion:

Numerical studies of MHD hybrid Nanofluid flow between coaxial cylinders demonstrate the potential to significantly improve heat transfer capabilities using hybrid Nanofluid and magnetic fields. This approach holds promise for a variety of industrial applications where efficient thermal management is important. Further research and development may lead to practical applications utilizing MHD and nanotechnology.

Chapter II. Problem definition and Mathematical modeling

Chapter II. Problem definition and Mathematical modeling

II.1 Introduction:

Flow fields (velocity components), thermal fields, pressure distributions, and local fluid properties all help explain a particular flow. A mathematical expression that represents the fundamental laws governing these variables. These equations are typically continuity equations representing the conservation of mass, Navier-Stokes equations representing the conservation of momentum, and energy equations representing the conservation of energy.

The values of several dimensionless groups determine how this set of governing equations is solved. We use the following numbers to divide these groups: Rayleigh, Richardson, Prandtl, Reynolds, Nusselt, and other dimensionless numbers are represented by various physical properties depending on the temperature.

II.2 Problem definition:

The current model features an annular pool formed by two coaxial cylinders. Within this annular space, the motion of the outer wall induces a rotating Nanofluid. The pool is influenced by a radial temperature gradient and a horizontal magnetic force. The nanofluid is created by dispersing copper nanoparticles (Cu) in kerosene oil, and a hybrid nanofluid is produced by combining Cu and graphene oxide (GO) nanoparticles, as detailed in Table 1. The focus is on the annular pool between the cylinders, with both axes aligned parallel to the z-axis. The outer cylinder rotates with an angular velocity (Ω), while the inner cylinder remains stationary. The annular region is defined by R = 1- (r_i/r_o), where *ri* and *r*o are the radii of the inner and outer cylinders, respectively. Numerical simulations are performed for specific parameters, including an aspect ratio A=H/ *r*o of 1, and an annular gap R=0.9. The simulations involve a constant application of a radial magnetic field B. The resulting magnetic field is negligible due to a magnetic Reynolds number (Rem) significantly less than one. Additionally, the outer cylinder acts as a heat source, maintaining a temperature T_h slightly higher than the inner wall temperature (T_c). Two scenarios are considered regarding the container walls: the first assumes electrical insulation, while the second assumes electrical conductivity of the inner and outer walls. The interplay of the magnetic field and thermal dynamics generates complex fluid flow and temperature distribution within the annular space, aiding in understanding the system's behaviour under these conditions. This setup is depicted in Fig. 1. The model makes several assumptions: laminar flow, the neglect of chemically active species such as Joule heating, thermal radiation, viscosity dissipation, and the Hall Effect. Both the base fluid and nanoparticles are maintained in thermal equilibrium. The nanoparticles, characterized by a

cylindrical shape (with n=6), are uniformly distributed throughout the Nanofluid. The hybrid Nano fluid consists of a (50% - 50%) mixture of GO-Cu nanoparticles suspended in kerosene oil (Table 2).

Table II- 1 Thermo-physical properties of different materials.

Substance	μ(kg/m.s)	Cp(J/kg.K)	K(W/m.K)	σ(S/m)	ρ(kg/m^3)	β(1/K)
Base fluid (Kerosene-oil)[27]	0.00164	2090	0.145	50	783	9.6×10^{-4}
Nanoparticle (Cu)[14]	-	385	401	5.96×10^{7}	8933	1.67×10^{-5}
Nanoparticle (GO) [26]	-	717	5000	6.3×10^{7}	1880	2.84×10^{-4}

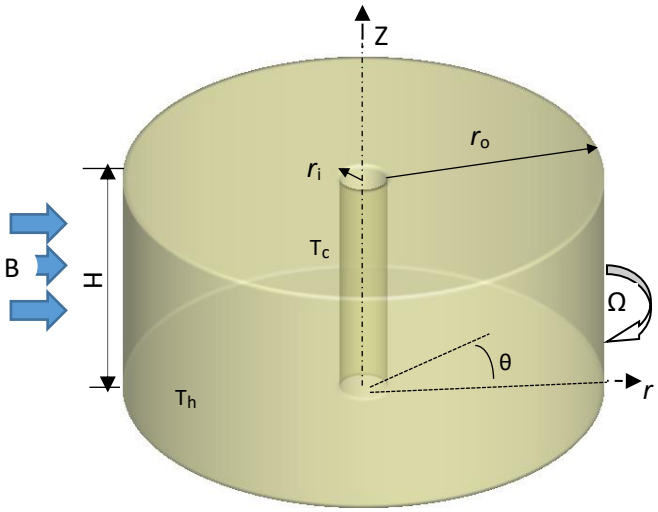

Figure.II. 1 Geometry of the problem.

II.3 Mathematical modeling:

Length, velocity, pressure, and electric potential are scaled byr_o,Ωr_o,$\rho_f(\Omega r_o)^2$, and$B_0\Omega {r_o}^2$, respectively, while the temperature is scaled as$\Theta = (\mathrm{T} - T_0)/\Delta\mathrm{T}$. Due to the moderate rotation rate, the flow remains steady. The governing equations, derived from references [14, 27, 29], are presented in dimensionless form as follows:

Law of conservation of mass:

$$\frac{1}{r}\frac{\partial(ru)}{\partial r}+\frac{1}{r}\frac{\partial w}{\partial \theta}+\frac{\partial v}{\partial z}=0 \qquad (II.\ 1).$$

Law of conservation of momentum:

$$u\frac{\partial u}{\partial r}+\frac{w}{r}\frac{\partial u}{\partial \theta}+v\frac{\partial u}{\partial z}-\frac{w^2}{r}=-\frac{\partial P}{\partial r}+\frac{1}{Re_f}\left(\frac{\mu_{hnf}\rho_f}{\mu_f\rho_{hnf}}\right)\left(\frac{1}{r}\frac{\partial}{\partial r}\left(r\frac{\partial u}{\partial r}\right)+\frac{1}{r^2}\frac{\partial^2 u}{\partial \theta^2}+\frac{\partial^2 u}{\partial z^2}-\frac{u}{r^2}-\frac{2}{r^2}\frac{\partial w}{\partial \theta}\right)+\left(\frac{\sigma_{hnf}\rho_f}{\sigma_f\rho_{hnf}}\right)\frac{{Ha_f}^2}{Re_f}F_{Lr}\ (II.\ 2).$$

$$u\frac{\partial v}{\partial r}+\frac{w}{r}\frac{\partial v}{\partial \theta}+v\frac{\partial v}{\partial z}=-\frac{\partial P}{\partial z}+\frac{1}{Re_f}\left(\frac{\mu_{hnf}\rho_f}{\mu_f\rho_{hnf}}\right)\left(\frac{1}{r}\frac{\partial}{\partial r}\left(r\frac{\partial v}{\partial r}\right)+\frac{1}{r^2}\frac{\partial^2 v}{\partial \theta^2}+\frac{\partial^2 v}{\partial z^2}\right)+\left(\frac{Ra_f}{Pr_f Re_f^2}\right)\left(\frac{(\rho\beta)_{hnf}}{\beta_f\rho_{hnf}}\right)\Theta+\left(\frac{\sigma_{hnf}\rho_f}{\sigma_f\rho_{hnf}}\right)\frac{{Ha_f}^2}{Re_f}F_{Lz} \qquad (II.\ 3).$$

Swirl equation:

$$u\frac{\partial w}{\partial r}+\frac{w}{r}\frac{\partial w}{\partial \theta}+v\frac{\partial w}{\partial z}-\frac{uw}{r}=-\frac{\partial P}{\partial \theta}+\frac{1}{Re_f}\left(\frac{\mu_{hnf}\rho_f}{\mu_f\rho_{hnf}}\right)\left(\frac{1}{r}\frac{\partial}{\partial r}\left(r\frac{\partial w}{\partial r}\right)+\frac{1}{r^2}\frac{\partial^2 w}{\partial \theta^2}+\frac{\partial^2 w}{\partial z^2}-\frac{w}{r^2}-\frac{2}{r^2}\frac{\partial u}{\partial \theta}\right)+$$

$$\left(\frac{\sigma_{hnf}\rho_f}{\sigma_f\rho_{hnf}}\right)\frac{{Ha_f}^2}{Re_f}F_{L\theta}(II.\ 4).$$

Law of conservation of energy:

$$\frac{\partial \Theta}{\partial \tau}+u\frac{\partial \Theta}{\partial r}+\frac{w}{r}\frac{\partial \Theta}{\partial \theta}+v\frac{\partial \Theta}{\partial z}=\frac{1}{Re_f Pr_f}\left(\frac{\alpha_{hnf}}{\alpha_f}\right)+\left(\frac{1}{r}\frac{\partial}{\partial r}\left(r\frac{\partial \Theta}{\partial r}\right)+\frac{1}{r^2}\frac{\partial^2 \Theta}{\partial \theta^2}+\frac{\partial^2 \Theta}{\partial z^2}\right) \qquad (II.\ 5).$$

Electric currents can be induced by the interaction of magnetic fields with convection, as explained by Faraday's law of electromagnetic induction. This phenomenon happens when an electromotive force (FM) and an electric current (J) are produced by the relative motion of a conductor (or conducting fluid) in a magnetic field. To describe the behaviour of the potential Φ, Ohm's law can be used in the following form:

$$\nabla^2\Phi=\nabla.(U\times\vec{e}_r) \qquad (II.\ 6).$$

$$\frac{1}{r}\frac{\partial}{\partial r}\left(r\frac{\partial \Phi}{\partial r}\right)+\frac{1}{r^2}\frac{\partial^2\Phi}{\partial \theta^2}+\frac{\partial^2\Phi}{\partial z^2}=-\frac{1}{r}\frac{(\partial rv)}{\partial r}+\frac{\partial u}{\partial z} \qquad (II.\ 7).$$

The dimensionless electric currents are given by:

$$\vec{j}=-\vec{\nabla}\varphi+U\times\vec{e}_r \qquad (II.\ 8).$$

The electromagnetic force (Lorentz force) may be found directly by:

$$F_M=\vec{J}X\vec{B} \qquad (II.\ 9).$$

$$F_{Lr}=0\ ,\ F_{L\theta}=B(\frac{\partial\Phi}{\partial z}-u)\ F_{Lz}=B\left(\frac{\partial\Phi}{\partial\theta}\right) \qquad (II.10).$$

The Rayleigh number (Raf), Reynolds number (Ref), Prandtl number (Prf), Hartmann number (Haf), and are dimensionless parameters that characterize the base fluid. These parameters are defined as:

$$\begin{cases} Re_f = \frac{\Omega r_o^2}{\nu_f} \\ Ra_f = \beta_f g \Delta T r_o^3 / \nu_f \alpha_f \\ Ha_f = Br_o \sqrt{\frac{\sigma_f}{\rho_f \nu_f}} \\ Pr_f = \nu_f / \alpha_f \end{cases} \quad (I.11).$$

Given the initial and boundary conditions, the velocity along all walls is assumed zero according to the no-slip conditions. Adiabatic conditions are applied to the upper and lower walls, and the outer (Th) and inner (Tc) boundaries of the axial cylinder maintain a constant temperature. In the case of electric potential, electrically insulated walls have their normal derivative set to zero, which guarantees that there is no electric current normal to the interface between the fluid and insulating walls. This implies that the potential of the upper and lower disks is determined by the condition $\partial\Phi/\partial z=0$. The boundary conditions for electric potential are closely related to the electrical characteristics of the wall, such as its conductivity and thickness (ew, σw), in cases where the inner and outer boundaries are electrically conductive. The formulation for the electric potential is given by reference [38].

$$J_r = -k_w \frac{\partial}{\partial r}(J_r) \quad (II.12).$$

$$-\frac{\partial \Phi}{\partial r} = -k_w \frac{\partial}{\partial r}\left(\frac{\partial \Phi}{\partial r}\right) \quad (II.13).$$

The magnetic boundary condition in the (EC-inner-outer) case after integration is as $\Phi = k_w \frac{\partial \Phi}{\partial r}$. In this scenario, the conductance ratio is represented by $k_w = \sigma_w e_w$/and R.

The local and average Nusselt numbers, denoted as distinguishes the heat transfer:

$$Nu(r,\theta) = \frac{k_{hnf}}{k_f}\left(\frac{\partial \theta}{\partial z}\right)\Big|_{z=0 \text{ or } H} And \overline{Nu} = \left(\frac{1}{\pi}\right)\int_0^1 \int_0^{2\pi} Nu\,(r,\theta) r d\theta dr \quad (II.14).$$

Table II- 2 Thermo-physical property [22, 27, and 39].

	Nano Fluid	hybrid nanofluid
Density	$\rho_{nf} = (1-\varphi)\rho_f + \varphi\rho_P$	$\rho_{hnf} = (1-\varphi_2)\left[(1-\varphi_1)\rho_f + \varphi_1\rho_{P1}\right] + \varphi_2\rho_{P2}$
Dynamic viscosity	$\mu_{nf} = \frac{\mu_f}{(1-\varphi)^{2.5}}$	$\mu_{hnf} = \frac{\mu_f}{(1-\varphi_1)^{2.5}(1-\varphi_2)^{2.5}}$
Heat capacity	$(\rho C_p)_{nf} = (1-\varphi)(\rho C_p)_f + \varphi(\rho C_p)$	$(\rho C_p)_{hnf} = (1-\varphi_2)\left[(1-\varphi_1)(\rho C_p)_f + \varphi_1(\rho C_p)_{P1}\right] + \varphi_2(\rho C_p)_{P2}$
Expansion coefficient	$(\rho\beta)_{nf} = (1-\varphi)(\rho\beta)_f + \varphi(\rho\beta)$	$(\rho\beta)_{hnf} = (1-\varphi_2)\left[(1-\varphi_1)(\rho\beta)_f + \varphi_1(\rho\beta)_{P1}\right] + \varphi_2(\rho\beta)_{P2}$
Conductivity	$k_{nf} = k_f\left[\frac{k_f + (n-1)k_f - (n-1)(k_f - k_p)\varphi}{k_p + (n-1)k_f + \varphi_1(k_f - k_p)}\right]$	$\frac{k_{hnf}}{k_{nf}} = \left[\frac{k_{P2} + (n-1)k_{nf} - (n-1)(k_{nf} - k_{p2})\varphi_2}{k_{p2} + (n-1)k_{nf} + \varphi_2(k_{nf} - k_{p2})}\right]$ Where $\frac{k_{nf}}{k_f} = \left[\frac{k_{P1} + (n-1)k_f - (n-1)(k_f - k_{p1})\varphi_1}{k_{p1} + (n-1)k_f + \varphi_1(k_f - k_{p1})}\right]$
Electrical conductivity	$\sigma_{nf} = \sigma_f\left[\frac{\sigma_p + 2\sigma_f - 2\varphi(\sigma_f - \sigma_p)}{\sigma_p + 2\sigma_f + \varphi(\sigma_f - \sigma_p)}\right]$	$\sigma_{hnf} = \sigma_{nf}\left[\frac{\sigma_{p2}+2\sigma_{nf}-2\varphi_2(\sigma_{nf}-\sigma_{p2})}{\sigma_{p2}+2\sigma_{nf}+\varphi_2(\sigma_{nf}-\sigma_{p2})}\right]$, Where $\sigma_{nf} = \sigma_f\left[\frac{\sigma_{p1}+2\sigma_f-2\varphi_1(\sigma_f-\sigma_{p1})}{\sigma_{p1}+2\sigma_f+\varphi_1(\sigma_f-\sigma_{p1})}\right]$

II.4 Boundary conditions:

The boundary conditions are as:

At the upper disk ($z = H/r_o,\ r_i/r_o \le r \le 1,\ 0 \le \theta < 2\pi$):

$U(u,v,w) = 0, \frac{\partial\Theta}{\partial z} = 0\ ,\ \frac{\partial\Phi}{\partial z} = 0,$

At the bottom disk ($z = 0,\ r_i/r_o \le r \le 1\ , 0 \le \theta \le 2\pi$):

$U(u,v,w) = 0, \frac{\partial\Theta}{\partial z} = 0\ , \frac{\partial\Phi}{\partial z} = 0$

At the stationary inner wall ($0 \le z \le H/r_o\ , r = r_i/r_o\ , 0 \le \theta \le 2\pi$):

$U(u,v,w) = 0\ , \Theta = 0;\ \frac{\partial\Phi}{\partial r} = 0$ where (EI-walls)), or $\Phi = k\frac{\partial\Phi}{\partial r}$ where (EC-inner)

At the rotating outer wall ($0 \le z \le d/r_o\ ,\ r = 1,\ 0 \le \theta < 2\pi$):

$u = v = 0,\ \ w = 1\ \ ,\ \Theta = 1\ , \frac{\partial\Phi}{\partial r} = 0$ where (EI-walls)), or $\Phi = k\frac{\partial\Phi}{\partial r}$, where (EC-outer)

Periodicity conditions for geometrical symmetry are $U(r;\theta;\ z) = U(r;\ \theta + 2\pi;\ z)$.

Chapter III. Numerical implementation and Grid testing

Chapter III. Numerical implementation and Grid testing

III.1 Introduction:

Computerized modelling is these days a basic way to think about diverse marvels and the improvement and enhancement of unused frameworks or forms. Numerous forms include characteristic convection streams of Nanofluid; their exact information may be a major resource for understanding the marvels displayed.

In this chapter, we will utilize the limited volume strategy as a strategy of discretization. The last-mentioned strategy comprises joining the fractional differential conditions on volumes encompassing each point of the work. Fathoming the condition framework permits us to decide the areas where all the factors of the issue are considered.

Within the fields of warm liquid mechanics and combustion, physical marvels are portrayed by unequivocally coupled and nonlinear halfway differential conditions (PDEs). In general, these conditions don't concede explanatory arrangements, but in exceptionally rearranged cases, a numerical arrangement may be conceivable by changing these differential conditions into frameworks of straight arithmetical conditions by a discretization strategy some time ago and recently fathoming this framework by coordinate strategies or by cycles. There are a few discretization strategies right now being utilized, for example:

- The finite difference method.
- The finite element method.
- The finite volume method.

In this chapter, we also carried out an advanced recreation utilizing the ANSYS Workbench program editor. This stage offers a diverse approach to the development of a demonstration by reusing the beginning ANSYS code. It is especially suited to case handling. Complex geometry (numerous bodies of parts) and users not experienced within the field of calculation. In this environment, the user works on the geometry and not on the show itself. The stage is hence dependable for changing over the questions entered by the client into ANSYS code some time ago, recently propelling the determination.

III.2 The finite volume method:

To apply the finite volume method to solve the problem, follow these steps:

- Define a study domain and divide this computational domain into a finite number of discrete control volumes. The sum is exactly equal to the volume of the computational domain. We say network.

- Discretization of various equations governing phenomena. In the end, we get a system of algebraic equations.
- Solve the final algebraic system using a solution method (iterative or direct).

The advantage of this method compared to other numerical methods is that it is conservative. That is, everything that goes out of one control volume goes into another control volume.

To illustrate the application of this method, consider the general transport equation written for the property Φ as follows:

$$\frac{\partial \rho \Phi}{\partial t} + div(\rho \Phi u) = div(\Gamma_\Phi grad\Phi) + S_\Phi \qquad (III.\ 15).$$

In other words:

$$\begin{pmatrix}\text{variation de } \Phi \text{ dans un} \\ \text{élément de fluide}\end{pmatrix} + \underbrace{\begin{pmatrix}\text{flux net de} \\ \text{l'élément de fluide}\end{pmatrix}}_{\text{terme convectif}} = \underbrace{\begin{pmatrix}\text{variation de } \Phi \text{due} \\ \text{à la diffusion}\end{pmatrix}}_{\text{terme diffusif}} + \underbrace{\begin{pmatrix}\text{variation de } \Phi \text{due} \\ \text{aux sources}\end{pmatrix}}_{\text{terme source}}$$

Such as:

Γ_Φ: the diffusion coefficient.

S_Φ: the source term.

The resolution of the equation by the finite volume method essentially lies in its integration over a control volume:

$$\int_{cv} \frac{\partial(\rho\Phi)}{\partial t} dv + \int_{cv} div(\rho\Phi u) dv = \int_{cv} div(\Gamma_\Phi grad\Phi) dv + \int_{cv} S_\Phi dv \qquad (III.\ 16).$$

III.3 Resolution steps using the finite volume method:

III.3.1 Mesh:

The computational space is partitioned into an arrangement of subdomains called control volumes. These control volumes encompass the whole calculation space, such that the whole of their volumes is precisely equal to the volume of the calculation space.

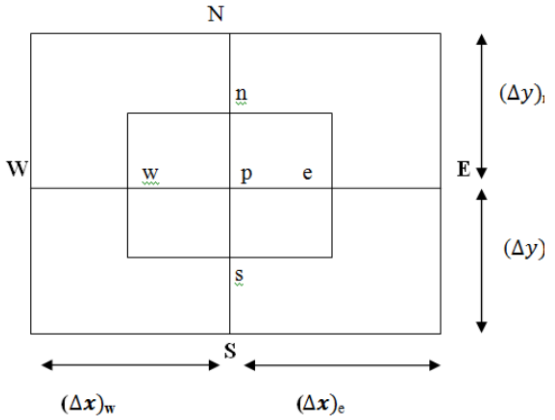

Figure.III. 1 Diagram of the control volume in the two-dimensional case.

The subordinate factors are put away in discrete focuses called hubs (focuses of crossing points of the work lines; see figure. (III.1). the hubs are numbered from 1 to Ni; taking after x, the hub (i, j) is called P; it is encompassed by the hubs E (East), N (North), W (West), and S (South). Each hub is related to a limited volume (fig. III-1); the faces of the volume are found within the centre between the hubs; the surface of VC comprises four planes, famous by lowercase letters compared to their headings e, w, n, and s (illustration: face w is within the centre between hubs W and P).

The remove increases Δx, Δy, Δxe, Δyn, Δxw, Δys are characterized in (fig. III.1). the scalars ϕ (pressure P, temperature T) are put away at the central hub. The speed components u and v are put away in moved hubs. The utilization of such entwining networks permits the calculation of weight angles within the energy conditions, without the insertion of weights and the calculation of convective streams within the conditions without the introduction of speeds.

III.3.2 Discretization:

Schemas used in the fluent part:

- **Pressure (Standard diagram):**

The pressure value is stored in the centre of the cell. For the surface pressure values required to solve the continuity equation, FLUENT offers several interpolation schemes, including the standard scheme.

Interpolation is done using the coefficients of the momentum equation. This method is suitable when pressure fluctuations between cell centres are small.

Given the issues of digital distribution, more accurate digital systems are being tested, such as this system based on two upstream connections.

The main problems encountered when discretizing the convective terms are the values of the transport properties Φ on the surface of the control volume and the calculation of the convective flow through these boundaries.

We introduced central differentiation to obtain the discretized equations of the diffusion and source terms. This technique can also be used for the convective term.

Unfortunately, while diffusion phenomena propagate properties and disperse these gradients in all directions, convection shows its influence only in the flow direction.

- **Pressure-speed coupling:**

The pressure, which acts through the components of its gradient, couples the equations of the components of momentum but we do not have an equation specific to this variable.

Patankar and Spalding's idea is to use the continuity equation to obtain the pressure field because if the appropriate pressure field is considered when working with the momentum equation, the resulting velocity will satisfy the continuity equation. Therefore, the latter seems to be the limit verified by the pressure field.

Three algorithms are considered by FLUENT to manage the speed-pressure link:

SIMPLE: «Semi Implicit Method for Pressure Linked Equations»: the most robust.

SIMPLE: «Semi Implicit Method for Pressure-linked Equations Consistent»: It gives faster convergence for simple problems.

PISO: « Pressure Implicit Solution by Split Operator»: it is useful for unstable flow problems.

The algorithm chosen in our study is the SIMPLE algorithm. When the calculation is initialized, a pressure field fixed a priori is introduced into the momentum balance equation, making it possible to calculate the first velocity field. The combination of the mass balance and momentum equations makes it possible to correct these first pressure and velocity fields. The other transport equations are then solved, and the corrected pressure field is used to initialize the calculation in the next iteration. This succession of operations is repeated until the convergence criteria are reached.

III.3.3 SIMPLE algorithm:

The discretisation of the transport-diffusion equation over the control volume by the finite volume method includes the values of the velocities at the interfaces of the volumes (Ue, Uw, Us, Un). Therefore, it is interesting to calculate these velocities directly at the interface (without performing interpolation). Contrarily, discretizing continuity equations and pressure gradients using linear interpolation can introduce significant errors because the "chequerboard" pressure or velocity distribution is assumed a uniform field. To avoid these issues, I prefer to use an offset grid. The main grid is constructed where pressure, temperature, and concentration are calculated. To calculate the horizontal and vertical velocity, two grids are used, shifted to the right and up, respectively.

The SIMPLE algorithm, an acronym for “Semi-Implicit Method for Pressure-Linked Equations," makes it possible to solve the system of discretized equations. This algorithm stipulates the existence of a relationship between the corrected velocities and the corrected pressures to verify the mass conservation equation.

The representative diagram of this iterative process is as follows:

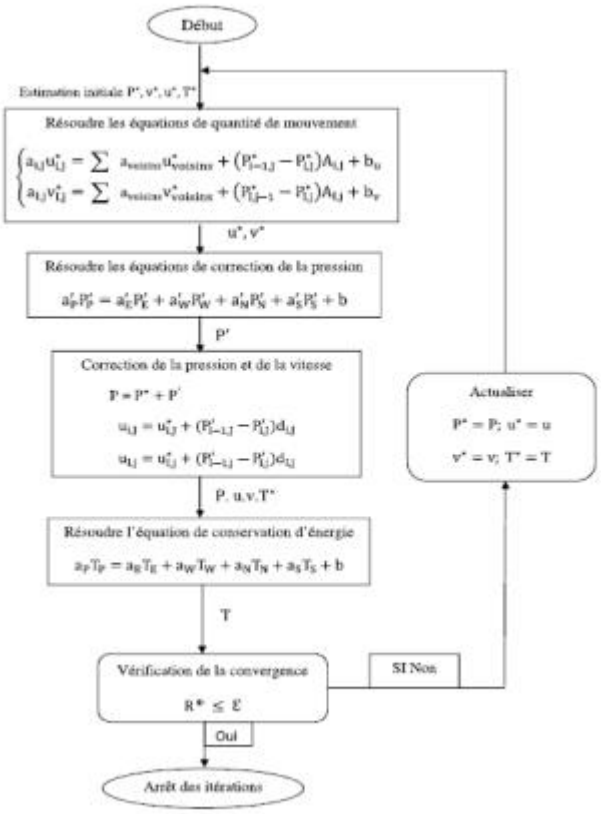

Figure.III. 2 Flowchart of the SIMPLE algorithm.

U and v are the two components of velocity vectors, and p represents the pressure. Φ* is defined by Φ = Φ* + Φ' is a correction.

III.3.4 Fluent:

It is written in C, and the overall numerical approach used starts with reading the geometry and mesh. Now let us move on to the type of solver for this case. This includes implicit formulation for the steady-state two-dimensional case, then discretization of the model equations in the Solve menu, solving the discretized system of equations, and finally a "separate" solver for post-processing. We initialize all four variables (pressure, two components of velocity, and temperature) that are computed at all points in the network. You then manage the progress of the iterations by monitoring the equation residuals associated with each variable. Therefore, under FLUENT, the work will consist of successively ensuring:

- The choice of equations processed.
- The description of the boundary conditions.
- Resolution management.
- Analysis of the results.

Fluent uses finite volume methods as a way to discretize equations that control flow, such as the continuity equation, momentum, and energy. We use this technique based on integral equations for the control volume.

The discretization schemes for the different variables are summarized in the table below:

Table III- 1 discretization scheme.

Variable	Plan
Pressure	Standard
Amount of movement	Off-centered upstream 2nd order
Energy	Off-centered upstream 2nd order
Pressure-speed coupling	Simple

III.3.5 Under relaxation:

Partial relaxation is regularly used in nonlinear problems to prevent divergence in iterative processes. The rate of change of variables from one iteration to the next is reduced by introducing the under-relaxation factor.

In our case, the sub-relaxation values are given in the following table:

Table III- 2 under-relaxation values.

Variable	Under-relaxation factors
Pressure	0.3
Amount of movement	0.7
Density	1
Energy	1

III.4 Numerical details used in this work:

The governing equations are discretized using the finite volume approach, enabling numerical solutions on a discrete grid. To be more precise, the diffusion components were estimated using the central difference approach, and the convective terms were managed using the QUICK technique [41]. Initially, (P), (u), (v), and (w) were determined by solving equations (1-4). Equation (5) was utilized to ascertain the temperature, and Eq. (7) was employed to calculate the potential (Φ). Until convergence was attained, this process was repeated. Using the SIMPLE algorithm, the relationship between pressure and velocity was addressed. The

tridiagonal matrix method (TDMA) is used to solve the discretized linear equations consecutively after they are converted into tridiagonal form.

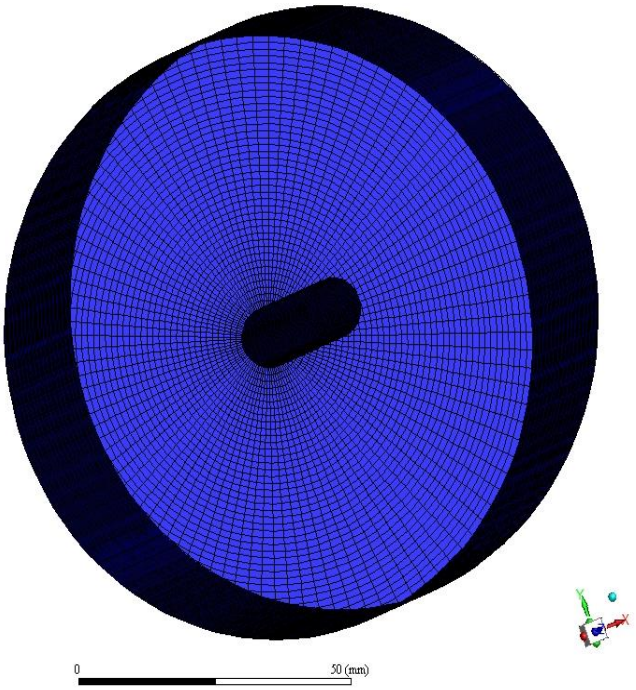

Figure.III. 3 Mesh.

Three different meshes were used for simulations to evaluate grid dependence. The Hartmann layers close to the walls became thinner as the Hartmann number (Ha) increased, roughly with a thickness of ~1/Ha. As such, non-uniform grids were used in simulations where Ha values were between 0 and 40. For Ha values between 0 and 5, a grid of 55×110×55 nodes was utilized; for Ha values beyond 5 and up to 10, a grid of 75×110×75 nodes; and for Ha values above 20, a grid of 85×110×85 nodes. We tested grid independence with three different Ha values: 0, 10, and 30. Table III.3 displays the grid arrangements and outcomes for every scenario.

The appropriateness of the selected grid was confirmed by comparing several values of the average Nusselt on the inner wall, which showed variations smaller than 3%. On a workstation with 128 GB of memory, numerical simulations were run. Convergence was deemed to have been reached at each time step when the largest residual error of the continuity equation was less than 10-6 for all control volumes.

Table III- 3 Validation of grid sizes.

Ha=0		Ha=10		Ha=30	
Mesh(r, θ, z)	$\overline{Nu}$	Mesh(r, θ, z)	$\overline{Nu}$	Mesh(r, θ, z)	$\overline{Nu}$
50×100×50	2.89	65×100×65	5.19	75×100×75	6.89
55×110×55	2.77	75×110×75	5.01	85×110×85	6.26
60×120×60	2.76	80×120×80	5.03	90×120×90	6.23

III.5 Conclusion:

Through this chapter, we briefly presented the finite volume method and the main steps to follow for this work. The resolution carried out by the FLUENT software gives results, which are presented in the following chapter.

Chapter IV. Results and discussion

Chapter IV. Results and discussion

IV.1 Introduction:

The interplay between an externally applied magnetic field and an electrically conducting fluid is crucial in magnetohydrodynamics (MHD). The Lorenz force causes the complicated interactions that result from the fluid functioning as a conductor and meeting the magnetic field. An insulating wall restricts the flow, and if the wall conducts electricity, it has a big impact on the dynamics of the system. This interaction produces two separate layers: the Robert layer near the insulating wall, which permits more mobility, and the Hartmann layer near the conductive wall, which resists fluid motion because of the magnetic field. Understanding the concept of electromagnetic stability is essential to comprehend the behaviour of conducting fluids in magnetic fields, particularly when it comes to spinning fluid systems. When a magnetic field is applied in a favourable direction, such as in small and moderate cylinders, it induces an electric current within the electrically conductive fluid. This phenomenon primarily occurs due to the Lorentz force, which arises from the interaction between the magnetic field and the moving charged particles within the fluid.

This section's main goal is to investigate how magnetic fields affect skin friction (Cf), temperature (Θ), azimuth velocity (w), and Nusselt number (Nu). There is a comparison between the magnetic damping effects seen in kerosene oil, a based fluid, and a hybrid Nanofluid. The simulations cover the case of fully electrically conducting inner-outer vertical walls (EC-inner-outer) and electrically insulating all walls (EI-Walls). Solid volume fraction (ϕ=0.01) nanoparticles are always used in all of the simulations that are run. Kerosene oil is used as the base fluid; it has a Prandtl number Pr = 21, and the Reynolds number is fixed at Re=1000. A cylinder with a height-to-radius ratio (H/R) of one contains the fluid.

IV.2 Validation:

A comparison with the numerical results of Alsaedi et al. [39] was made, as Figure 1 shows. In the context of a numerical study on the flow of a hybrid nanofluid consisting of graphene oxide (GO) and copper (Cu) nanoparticles in a Kerosene oil base fluid between two coaxial cylinders, this assessment looks at the effects of magnetic parameters and volume fraction for two values (ϕ=0.01 and 0.04) on skin friction (Cf). The comparison shows that Cf increases with higher magnetic fields and volume fractions. With a maximum difference of less than 1%, which is considered insignificant for a numerical analysis, the results show that the derived values are in good agreement with one another.

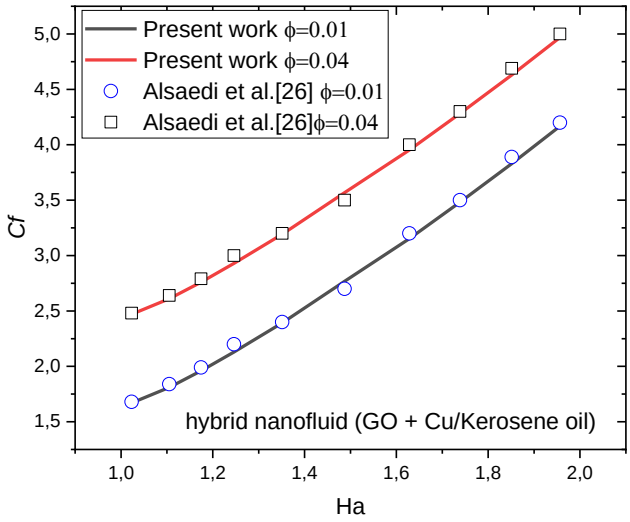

Figure.IV. 1 Comparison with (a) the numerical result of Alsaedi et al. [26], which gives Ha and ϕ on via Cf.

IV.3 Electrically insulating container walls:

When every wall of the coaxial cylinder is insulating, the electric current lines inside the fluid form closed loops. The Hartmann layers predominantly concentrate on the inner-outer walls in this configuration. A radial magnetic field's presence induces alterations in the Nanofluid's convection. This effect is attributed to the Hartmann layers near the inner and outer walls, along with the development of Roberts's layers near the bottom and top walls. The observed changes in convection inside the Nanofluids are a result of the interaction between these layers and the radial magnetic field.

Figure. 2 displays the case without a magnetic field (Ha=0), providing insight into the temperature profile at r=0.2 and the local Nusselt number at the inner wall. The plot encompasses three fluids: Kerosene oil, nanofluid (Cu/ Kerosene oil), and hybrid nanofluid (GO- Cu/Kerosene oil). It is observed that the fluid change does not significantly alter the temperature distribution profile. However, it should be noted that for the hybrid nanofluid, higher temperature values compared to the other two fluids are observed near the inner wall of the cylinder Figure. 2b compares three fluids via the local Nusselt number plotted at the inner wall (θ=0). The close positioning of local Nusselt lines is observed, suggesting that the enhancement in heat transfer may not be deemed significant. However, it is noteworthy that marginal improvements in thermal transfer are demonstrated by the hybrid nanofluid when compared to the other fluids.

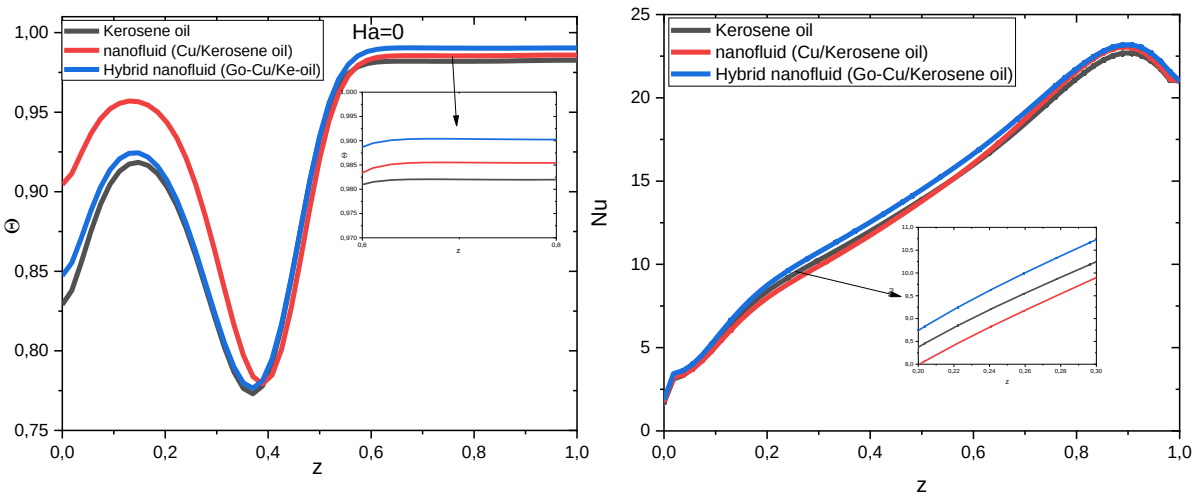

Figure.IV. 2 Case Ha= 0 (Without magnetic field): Temperature profile (left), local Nusselt (right).

Figure. 3a illustrates the impact of the Hartmann number (Ha) on the azimuthal velocity (w) of both nanofluid (Cu/Kerosene oil) and pure Kerosene oil at a radial distance of r=0.2. W increases with higher Ha values. The increase in w is more pronounced in the nanofluid (Cu/Kerosene oil) case than in pure Kerosene oil. In Figure. 3b, the distribution of azimuthal velocity at r=0.2 is presented for the nanofluid (Cu/Kerosene oil) with varying Ha values (0, 10, 20, and 40). In the absence of a magnetic field, w appears as an arc with relatively small values compared to the higher Ha values. However, with an increase in Ha, w shows a significant rise. This phenomenon is attributed to the interaction between the external radial magnetic field and the beyond forces, leading to increased azimuthal velocity.

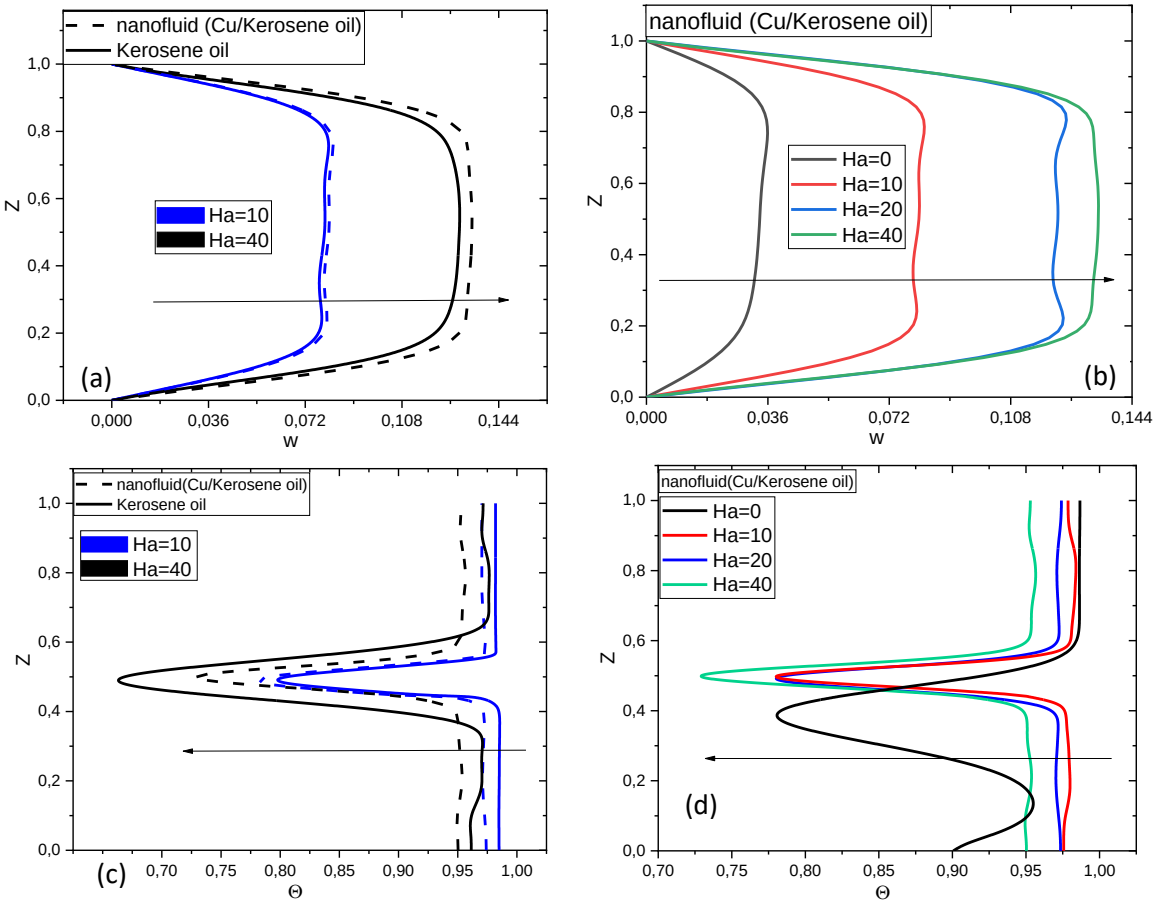

Figure. IV. 3 Impact of Ha on azimuthal velocity (top) and temperature (below) at r=0.2.

Figure 3c presents a comparison of the effects of two Hartmann numbers, Ha=10 and Ha=40, on the dimensionless temperature (Θ) of pure Kerosene oil and nanofluids (Cu/Kerosene oil). Θ displays a V-shaped pattern in this illustration, with higher values found at the top and bottom walls. When pure Kerosene is used instead of the nanofluid (Cu/Kerosene oil), there is a more noticeable increase in Θ. The distribution of Θ at r=0.2 for the nanofluid (Cu/Kerosene oil) with different Ha values is shown in Figure. 3d. Θ does not show symmetry about z=1/2 in the absence of a magnetic field. Nevertheless, when Ha rises, Θ becomes symmetric about the circular pool centre. The effects of the magnetic fields on Θ (Figure. 3d) contrast with those on azimuthal velocity (w), as shown in Figure. 3b. The temperature distribution at r=0.2 demonstrates that an increase in the Hartmann number leads to a reduction in both the minimum and maximum values of Θ.

For a deeper understanding of this phenomenon, Fig. 5 depicts the spatial temperature structure at Θ = 0.95. A comparison between Kerosene oil and hybrid nanofluid when Ha=0

reveals that the highest temperature emerges in the central region, resembling a spinning top iso-surface. With increasing Hartmann number (Ha=20), subtle changes are observed for Kerosene oil, while the shape undergoes a complete transformation for the hybrid nanofluid. This transformation may be attributed to the weakening of buoyant forces, countered by the intensified Lorentz force, particularly pronounced due to the development of Hartmann layers near the inner and outer walls.

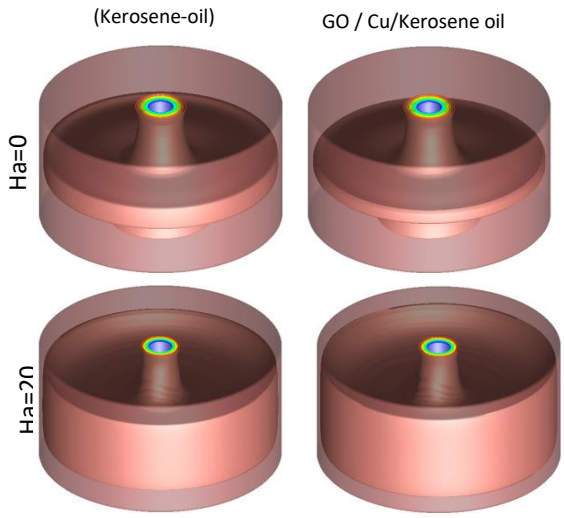

Figure.IV. 4 Spatial structure of temperature for the iso-value Θ = 0.95.

Figure 5a compares pure kerosene oil with a nanofluid composed of copper (Cu) and kerosene oil, showing the effect of the Hartmann number (Ha) on the local Nusselt number at the inner wall (θ = 0). However, the results show that for both pure kerosene oil and hybrid nanofluids (copper oil/kerosene), the Nusselt number increases with increasing Ha. On the other hand, the nanofluid (copper oil/kerosene) improved further. Heat transfer in the system occurs when a Lorentz is created between the fluid and the magnetic field. In Figure. 5a, it is observed that the effect of Ha on the Nusselt reaches a maximum at z=0.1 and z=0.9, respectively, and gradually decreases towards the centre of the toroidal complex. Various intensities of Ha ranging from zero to 40 are applied to the nanofluid (Cu + Kerosene oil) to measure the local Nusselt number at r=0.2, as depicted in Figure. 5b. At Ha=0, an asymmetric Nu profile with a lower value is observed. Moreover, Nu is found to rise with increasing magnetic intensity, resulting in an axisymmetric shape concerning z=1/2.

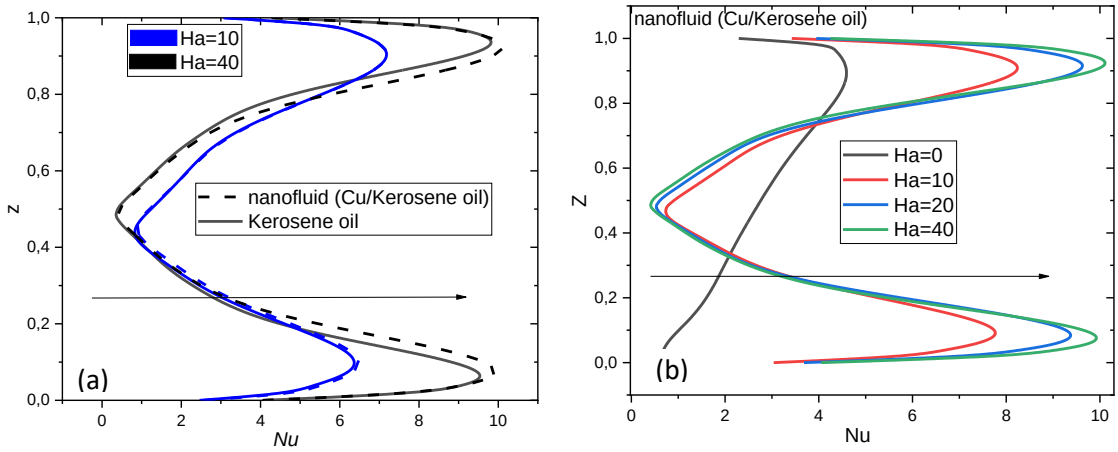

Figure.IV. 5 Affect of Ha on Local Nusselt number at the inner wall (θ=0) at r=0.2.

Figure. 6a illustrates the comparison of the skin friction coefficient (Cf) at the inner wall (θ=0) for pure nanofluid (Cu/Kerosene oil) and base fluid at two different Hartmann number values (Ha=10 and 20). Higher Ha values improve the coefficient for the pure base fluid as well as the nanofluid (Cu/Kerosene oil). Additionally, a predominant trend favouring nanofluid (Cu/Kerosene oil) is noted. In Figure. 6b, the skin friction coefficient is plotted at the inner wall with varying Ha intensities. At Ha=0, the profile appears as an arc with a small value. Furthermore, Cf rises from Ha=10 to 40, producing an axisymmetric profile that reflects the Nusselt profile about z=1/2. Notably, for z=0.15 and z=0.85, the highest values are attained.

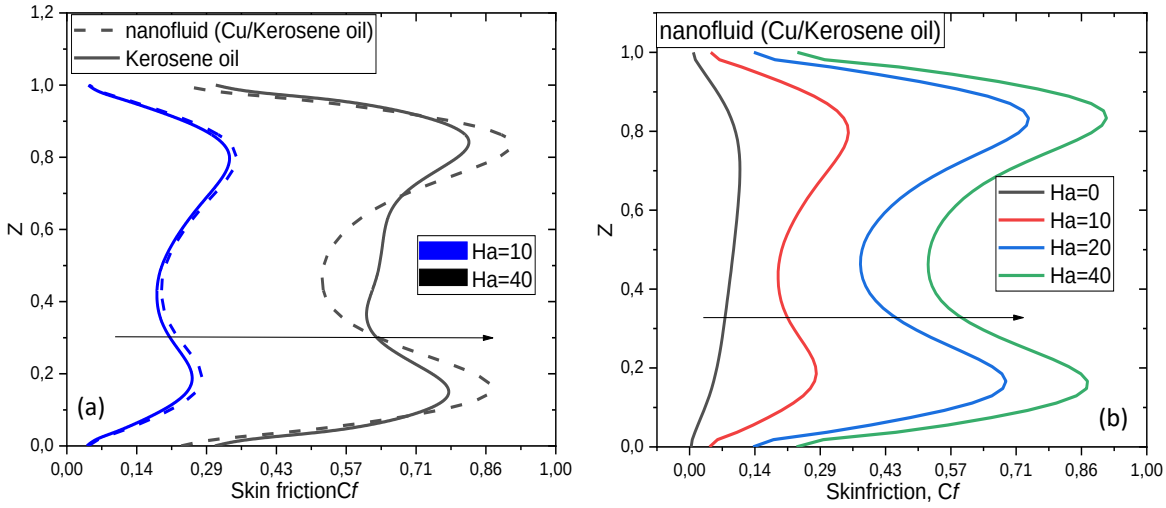

Figure.IV. 6 Skin friction at the inner wall (θ=0).

For more details, Figure 7 illustrates the influence of increasing the magnetic field intensity from 10 to 40. The profile of dimensionless temperature and azimuthal velocity w plotted r=0.2 shows that increasing Ha has a double effect; one increases the velocity and

decreases the temperature. The rise in azimuthal velocity (w) is more significant in the case of the nanofluid (Cu/kerosene oil) compared to the hybrid nanofluid. Conversely, the temperature reduction is more pronounced in the hybrid nanofluid than in the Nanofluid.

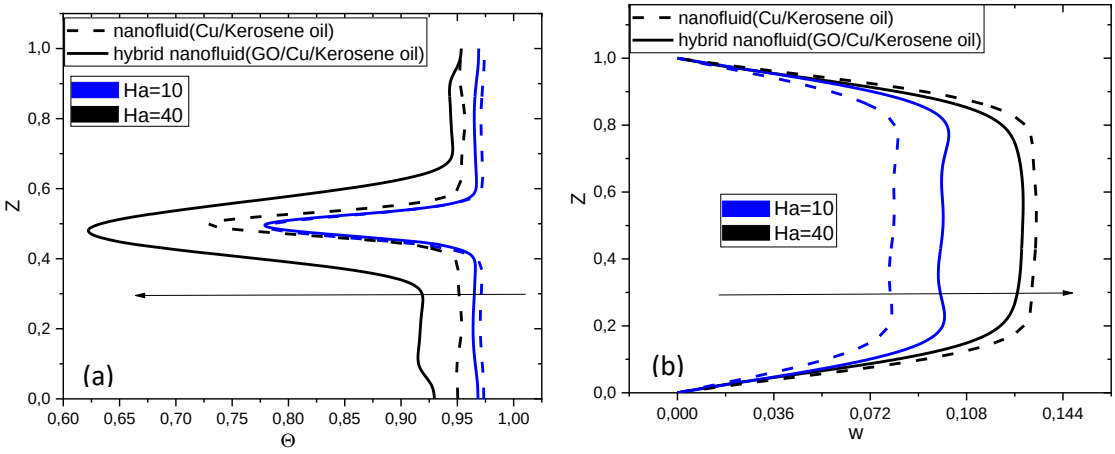

Figure.IV. 7 (a) Dimensionless temperature and (b) Azimuthal velocity w at r=0.2.

Figure 8a plots the skin friction coefficient comparison between nanofluid and hybrid nanofluid for Ha=10 and 40. When Ha=10, the profile takes the form of the letter M with a tiny value, and the hybrid nanofluid exhibits a greater rise in skin friction (Cf) than the nanofluid (Cu/kerosene oil). Cf rises and attends to the maximum levels at z = 0.2 and z = 0.8 heights with Ha = 40. On the other hand, the Cf is more noticeable in the nanofluid than in the hybrid nanofluid for the chosen value.

They are comparing a hybrid nanofluid with a copper nanofluid, Figure. 8b shows how the Hartmann number (Ha) affects the local Nusselt number at the inner wall (θ=0). For both nanofluids, the observation indicates that the Nusselt number rises as Ha rises. Interestingly, at Ha=10, the hybrid nanofluid shows a greater enhancement, and at Ha=40, the values for both nanofluids are about the same. An interesting finding is that the Nusselt profile is similar to the profile of the skin friction coefficient, peaking at the same elevations (z=0.2 and z=0.8) and toughing out at the middle (Z=1/2).

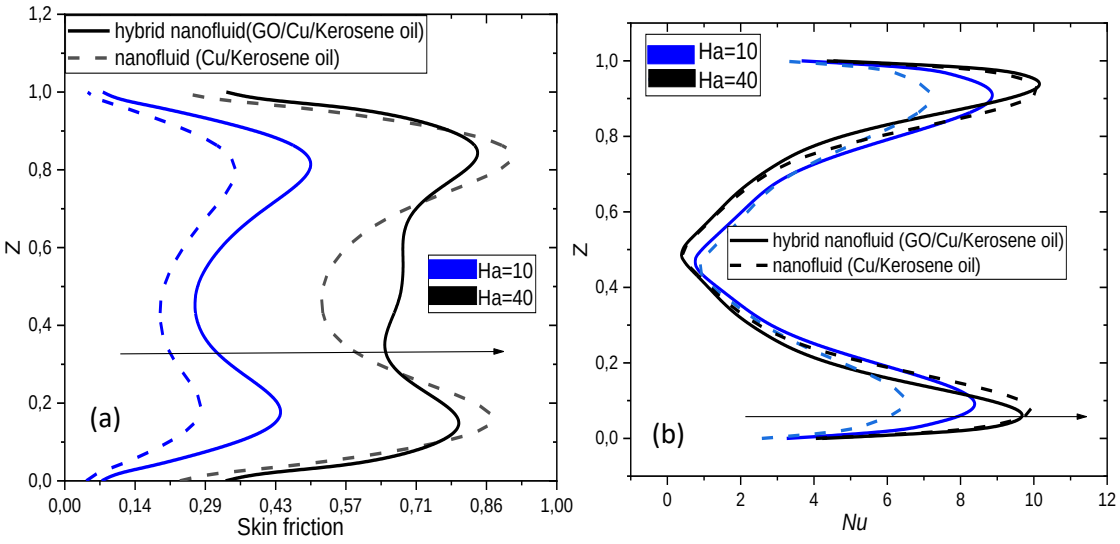

Figure.IV. 8 (a) Skin friction and (b) Nusselt number at the inner wall (θ=0).

IV.4 Electrically conducting inner-outer walls:

To delve deeper into the impact of electrical conductivity on convection in hybrid nanofluids under a magnetic field, we assume ideal electrical conductivity for the inner and outer walls of the enclosure, except for the bottom and top disks. Under this assumption, according to the thin wall theory, the electric potential remains constant across the wall, indicating that the wall current density is tangential. It is important to highlight that the introduction of electrical conductivity to the inner and outer walls eliminates the presence of the Hartmann layer, allowing the fluid to move under the influence of inertial forces.

Electrically conducting inner-outer walls (EC) and electrically insulating walls (EI) are the two examples that are compared in Figure. 9, for the values Ha=10 and Ha=20. Plotting the profile of azimuthal velocity w (Figure. 9b) and dimensionless temperature (Figure. 9a) at r=0.2 demonstrates that increasing Ha has two effects: one increases velocity and the other lowers the temperature. Based on observations, the temperature profile shows two peaks with θ=0.42 at z=0.1 and Z=0.9 in the case with (EC) and Ha=20. As opposed to this, a single peak with θ=0.2 is seen at z=0.5 in the case of (EI). There are two peaks in the dimensionless azimuthal velocity profile for Ha=10 and Ha=40, respectively, in the case of (EC). When compared to the CAS of (EC), the profile of w creates an arc with small values.

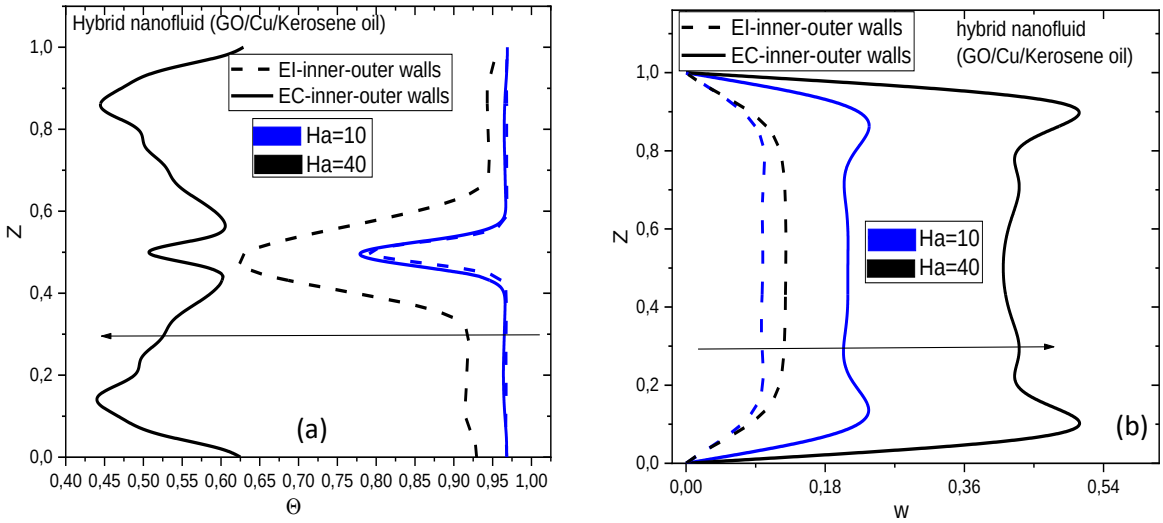

Figure.IV. 9 (a) Dimensionless temperature and (b) Azimuthal velocity w at r=0.2.

Fig.10 represents the evaluation of the average Nusselt as a function of Ha. With electrically conductive walls, the impact of the buoyancy force intensifies as the Hartmann number increases, resulting in an increasingly significant interaction between the viscosity and buoyancy forces with increasing Ha. Therefore, it is inferred that the combined effects of the magnetic field intensity and the electrical conductivity of the interior and exterior walls increasingly

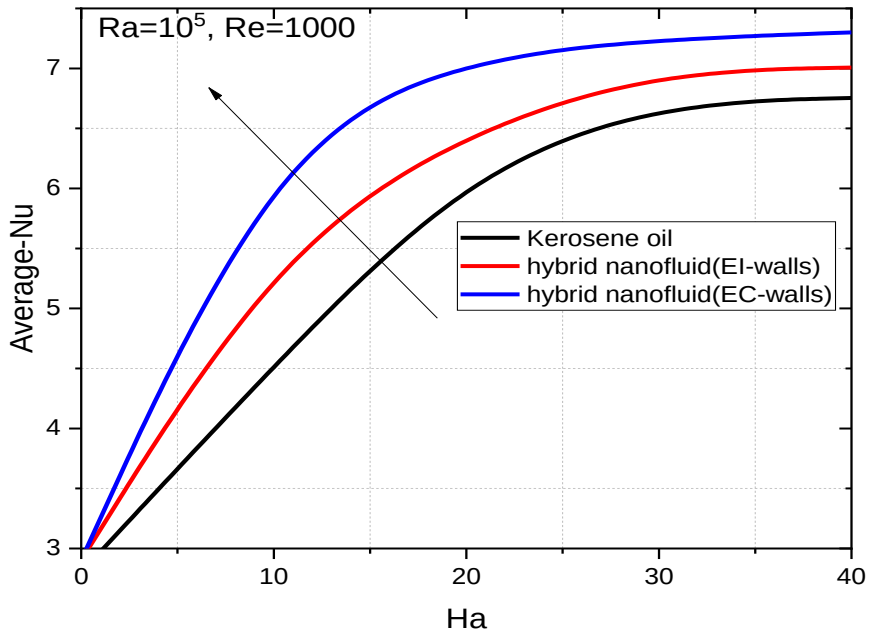

Figure.IV. 10 Average Nusselt number versus Hartmann number at the inner wall.

IV.5 Conclusions:

The following are the study's principal points:

- Lower fluid velocities are associated with stronger magnetic fields. With a hybrid Nanofluid, this drop is more pronounced.
- Higher Brikman numbers and greater magnetic fields cause the temperature of the Nanofluids to rise. For hybrid Nanofluid, the increase is greater.
- Lower fluid temperature is the effect of a higher Cu volume fraction.
- For greater magnetic fields, fluid pressure rises.
- Higher volume fractions and greater magnetic fields cause an increase in skin friction.
- Larger volume fractions increase the Nusselt number, while larger Brinkman numbers and stronger magnetic fields cause it to decrease.

General Conclusion

General Conclusion

The numerical study is centred on the whirling Nanofluid flow caused by the outer wall rotation of coaxial cylinders. A radial magnetic field and bidirectional temperature gradients are applied to the system. The transport equations are numerically solved using the finite-volume approach. Isotherms, velocity profiles, skin friction coefficients, and average Nusselt numbers are used to compare three distinct fluids: kerosene oil, Nanofluid (Cu-kerosene oil), and hybrid Nanofluid (GO-Cu/kerosene oil). The following summarizes the study's main conclusions:

- The temperature distribution remains unchanged in the absence of a magnetic field, and the Nanofluid hybrid's improved heat transmission is just 10%.
- The symmetrical surface temperature distribution of the Nanofluids is improved in the presence of a magnetic field, with a higher increase observed for the hybrid Nanofluid.
- Higher magnetic fields cause azimuthal velocities to be elevated at the centre of the container. Particularly in the instance of the hybrid Nanofluid, this rise is more noticeable.
- Skin friction increases with increasing magnetic field strength. As seen in both Nano fluid situations, it doubles with a doubling of the magnetic field's strength.
- When there is electrical conductivity in both the inner and outer walls, the hybrid Nano fluid provides a 60% improvement in heat transmission, which is optimal.
- Additional investigation employing an axial magnetic field and electrically conductive walls within a narrow annulus may enhance the process of heat transfer.

References

References:

[1] S.U.S. Choi, J.A. Eastman, Enhancing thermal conductivity of fluids with nanoparticles: The Proceedings of the 1995 ASME International Mechanical Engineering Congress and Exposition, San Francisco, USA, ASME, FED 231/MD, 66 (1995) 99-105.

[2] J.A. Eastman, S.U.S. Choi, S. Li, W. Yu, L.J. Thompson, Anomalously increased effective thermal conductivities of ethylene glycol-based nanofluids containing copper nanoparticles, Appl. Phys. Lett. 78 (6) (2001) 718–720.

[3] J. Sarkar, P. Ghosh, A. Adil, A review on hybrid nanofluids: recent research, development and applications, Renew. Sustain. Energy Rev. 43 (2015) 164–177.

[4] V. Trisaksri et S. Wongwises, Critical review of heat transfer characteristics of nanofluids, Renewable and Sustainable Energy Reviews, vol.11, N° 3, pp. 512 - 523, 2007.

[5] R. L. Hamilton ET O. K. Crosser, Thermal conductivity of heterogeneous two-component system. Industrial & Engineering Chemistry Fundamentals, Vol. 1, N°3, pp. 187- 191, 1962.

[6] J. A. Eastman, S. R. Phillpot, S. U. S. Choi, ET P. Keblinski, Thermal transport in nanofluids. Annual Reviews Materials Research, Vol. 34, pp. 219 - 246, 2004.

[7] S. E. Maïga, C. T. Nguyen, N. Galanis, ET G. Roy, Heat transfer enhancement in forced Convection laminar tube flow by using nanofluids. ICHMT International Symposium on Advances in Computational Heat Transfer, G. de Vahl Davis and E. Leonardi (Eds.) CDROM Proceedings, ISBN 1-5670-174-2, Begell House, New York, April 2004.

[8] X. Q Wang, A. S. Mujumdaret C. Yap, Thermal characteristics of tree-shaped microchannel nets for cooling of a rectangular heat sink. International Journal of Thermal.

[9] H.F. Oztop et E. Abu-Nada, Numerical Study of Natural Convection in Partially Heated Rectangular Enclosures Filled with Nanofluids, International Journal of Heat and Fluid Flow, Vol. 29, N°5, pp. 1326 - 1336, 2008.

[10]Bhattad A., Sarkar J. etGhosh P. (2017), Improving the Performance of Refrigeration Systems by Using Nanofluids: a Comprehensive Review, Renewable and Sustainable Energy Review, 82: 3656-3669.

[11] KLALECHE Sofiane MADJOUR Abderrahmane, "Simulation Numérique De La Convection Forcée Entre Deux Disques En Présence D'un Nano fluide", UNIVERSITE MOULOUD MAMMERI DE TIZI-OUZOU, (2015).

[12] Hamdi Moumni, Hedia Welhezi, Ridha Djebali, Ezeddine Sediki, "Accurate finite volume investigation of Nanofluid mixed convection in a two-sided lid-driven cavity including discrete heat sources"Univ. Tunis El-Manar, Tunisia, (2015).

[13] M. El Hafad Bara, Mme. Sakina El Hamdani, **M. A. Bendou, M. Karim Limam,**"Etude Numérique De La Convection Naturelle Du Mélange Eau-Cu Dans Une Cavité Partiellement Chauffée ", Université De La Rochelle, Av. Michel Crépeau, 17042 La Rochelle Cedex 1, France, (2017).

[14] Mahfoud, B., "Enhancement Heat Transfer of Swirling Nanofluid Using an Electrical Conducting Lid", *Journal of Thermophysics and Heat Transfer*, Vol 37, No.1, 2023, pp. 263–271 DOI: 10.2514/1.T6550

[15] Halelfadl, S. and Maré, T., "Thermal conductivity of CNT water-based nanofluids: *Experimental trends and models overview*," Vol.1, No.2, 2015, pp. 381- 390, https://doi.org/10.18186/jte.92293

[16] Kolsi, L., Alrashed, A., Al-Salem, K., Oztop, H.F., "Control of natural convection via inclined plate of CNT-water nanofluid in an open-sided cubical enclosure under magnetic field," *International Journal of Heat and Mass Transfer*, Vol.111, 2017, pp. 1007–1018, https://doi.org/10.1016/j.ijheatmasstransfer.2017.04.069

[17] Sheikholeslami, M., Mehryan, S.A.M., Shafee, A., Sheremet, M.A., "Variable magnetic forces impact on magnetizable hybrid nanofluid heat transfer through a circular cavity," *Journal of Molecular Liquids*, Vol. 277, 2019, pp. 388–396, https://doi.org/10.1016/j.molliq.2018.12.104

[18] Ghadikolaei, S.S., Hosseinzadeh, K., Ganji, D.D., "Investigation on ethylene glycol water mixture fluid suspend by hybrid nanoparticles (TiO2-CuO) over rotating cone with considering nanoparticles shape factor," *Journal of Molecular Liquids*, Vol. 272, 2018, pp. 226–236. https://doi.org/10.1016/j.molliq.2018.09.084

[19] Ruhani B., Toghraie D., Hekmatifar M., Hadian M., "Statistical investigation for developing a new model for rheological behaviour of ZnO–Ag (50%–50%)/Water hybrid Newtonian nanofluid using experimental data," *Physica A: Statistical Mechanics and its Applications*, Vol. 525, 2019, pp. 741–751, https://doi.org/10.1016/j.physa.2019.03.118

[20] Esfe, M.H., Esfandeh, S., Amiri, M.K., Afrand, M., "A novel applicable experimental study on the thermal behaviour of SWCNTs (60%)-MgO (40%)/EG hybrid nanofluid by focusing on the thermal conductivity," *Powder Technology*, Vol. 342, 2019, pp. 998–1007. https://doi.org/10.1016/j.powtec.2018.10.008

[21] Moradi, A. Toghraie, D., Isfahani, A.H.M., Hosseinian, A., An experimental study on MWCNT–water nanofluids flow and heat transfer in a double-pipe heat exchanger using porous media, *Journal of Thermal Analysis and Calorimetry*, 137, 2019, 1797–1807, https://doi. org/10.1007/s10973-019-08076-0.

[22] Mahmood, Z. , Iqbal, Z. , Ahmed Alyami, M., Alqahtani,B. , F Yassen, M., and Khan, U, "Influence of suction and heat source on MHD stagnation point flow of ternary hybrid nanofluid over convectively heated stretching/shrinking cylinder," *Advances in Mechanical Engineering*, Vol., 14, 2022, pp. 1–17, DOI:10.1177/16878132221126278

[23] Khan, M., Tahir, M.N., Adil, S.F., Khan, H.U., Siddiqui, M.R., Kuniyil, M., Tremel, W., "Graphene-based metal and metal oxide nanocomposites: Synthesis, properties and their applications." *Journal of Materials Chemistry A*, Vol. 3, 2015, pp. 18753–18808, doi: 10.1039/c5ta02240a.

[24] Ghadikolaeia, S.S., Gholiniab, M., "3D mixed convection MHD flow of GO- MoS2 hybrid nanoparticles in H2O– (CH2OH)2 hybrid base fluid under effect of H2 bond," *International Communications in Heat and Mass Transfer*, Vol. 110, 2020, 104371 Doi:10.1016/j.icheatmasstransfer.2019.104371

[25] Madani, F, Mahfoud B, Mahfoud Hibet E., "Influences of electrical conductivity of the cylindrical walls on heat transfer enhancement of nanofluid swirling flow" *International Journal of Thermofluid Science and Technology*, Vol. 10, 2023, Paper No. 100201, https://doi.org/10.36963/IJTST.2023100201

[26] Mahfoud, B., "Magnetic Field Effect on Natural Convection in Trapezoidal Geometry"**, https**://www.researchgate.net/publication/369040424, 2023, DOI: 10.13140/RG.2.2.27975.57761

[27] Mahfoud, B. "Simulation of Magnetic Field Effect on Heat Transfer Enhancement of Swirling Nanofluid" International *Journal of Computational Materials Science and Engineering*, Vol. 11, No. 4, 2022, 2250007, DOI: 10.1142/S2047684122500075.

[28] Mahfoud, B., Bendjaghloli, A., "Natural convection of a nanofluid in a conical container," Journal of Thermal Engineering, Vol. 4, 2018, pp. 1713-1723. DOI: 10.18186/journal-of-thermal-engineering.367407

[29] Mahfoud, B. "Effect of Wall Electrical Conductivity on Heat Transfer Enhancement of Swirling Nanofluid-Flow," *Journal of Nanofluids*, Vol. 12, 2023, pp. 418-428, https://doi.org/10.1166/jon.2023.1932

[30] Mollamahdi, M., Abbaszadeh, M., Sheikhzadeh, G. A., "Flow field and heat transfer in a channel with a permeable wall filled with Al2O3-Cu/water micropolar hybrid nanofluid, effects of chemical reaction and magnetic field," *Journal of Heat and Mass Transfer Research*, Vol.3, 2016, pp. 101- 114.

[31] Mansour, M.A., Sadia, S., Gorla, R., Rashad, A.M., "Effects of heat source and sink on entropy generation and MHD natural convection of Al2O3-Cu/water hybrid nanofluid

filled with a square porous cavity," *Thermal Science and Engineering Progress*, Vol.6, 2017, pp. 57-71.

[32] Mahfoud, B. "Magnetohydrodynamic effect on vortex breakdown zones in coaxial cylinders," *European Journal of Mechanics-B/Fluids*, Vol.89, 2021, pp. 445–457**.** https://doi.org/10.1016/j.euromechflu.2021.07.007 0997-7546

[33] Benhacine H., Mahfoud, .B, Salmi, M., 2021. "Stability effect of an axial magnetic field on fluid flow bifurcation between coaxial cylinders". *International Journal of Computational Materials Science and Engineering*, 2021, 2150023, DOI: 10.1142/S2047684121500238

[34] Mahfoud B., Benhacine H., Laouari A., Bendjaghlouli A., "Magnetohydrodynamic Effect on Flow Structures Between Coaxial Cylinders Heated from Below", *Journal Thermophysics and Heat Transfer*, Vol.34, No.2, 2019 pp. 1-10.https://doi.org/10.2514/1.T5805

[35] Mahfoud B., Laouari A., Hadjadj A., Benhacine H., "Counter-rotating flow in coaxial cylinders under an axial magnetic field", *European Journal of Mechanics-B/Fluids*, Vol. 78, 2019, pp.139-46.
https://doi.org/10.1016/j.euromechflu.2019.06.009

[36] Azzoug, M. O., Mahfoud, B., Mahfoud, Hibet. E., "Influence of External Magnetic Field on 3D Thermocapillary Convective Flow in Various Thin Annular Pools Filled with Silicon Melt," Journal of Applied Fluid Mechanics, Vol. 16,2023, pp. 1853-1864, Doi:10.47176/JAFM.16.09.1813

[37] Moussaoui, M., B.Mahfoud, Mahfoud, Hibet E., "Using a Magnetic Field to Reduce Thermocapillary Convection in Thin Annular Pools," Journal of Thermophysics and Heat Transfer, Vol.37, *No.4*, 2023, https://doi.org/10.2514/1.T6832

[38] Mahfoud, B., AZZOUG, O.M., "MHD effect on the thermocapillary silicon melt flow in various annular enclosures, "Crystal *Research & Technology*, Vol. 58, No.6, 2023, Doi: 10.1002/crat.202300025

[39] Alsaedi, A., Muhammad, K., Hayat, T., "Numerical study of MHD hybrid nanofluid flow between two coaxial cylinders" *Alexandria Engineering Journal*, Vol. 61, 2022, pp. 8355–8362, https://doi.org/10.1016/j.aej.2022.01.067

[40] Shahzad, F., Jamshed, W., R. Eid, M., M. El Din, S., Banerjee, R., "Mathematical modelling of graphene-oxide/ kerosene oil nanofluid via radiative linear extendable

surface," *Alexandria Engineering Journal*, Vol. 70, 2023, pp. 395–410, https://doi.org/10.1016/j.aej.2023.02.034

[41] Benhacine H., Mahfoud B., Salmi M., "Stability of conducting fluid flow between coaxial cylinders under thermal gradient and axial magnetic Field", *International Journal of Thermofluid Science and Technology*, Vol.9, 2022, No. 090202, https://doi.org/10.36963/IJTST.2022090202

[42] Benhacine H., Mahfoud B., Salmi M., "Stability of an Electrically Conducting Fluid Flow between Coaxial Cylinders under Magnetic field", *Journal of Applied Fluid Mechanics*, 2022, Vol. 15 (2), pp. 1741-1753. DOI: 10.47176/JAFM.15.02.33050